DESIGN, FABRICATION AND CHARACTERIZATION OF ANTENNA ARRAY FOR NEXT GENERATION 802.11AC WI-FI APPLICATION

Submitted by:

Syeda Areeba Nasir

NUST201260532MPNEC45312F

Supervised by:

Dr. Khawaja Bilal Ahmed Mahmood

THESIS
Submitted to:
Department of Electronic and Power Engineering
Pakistan Navy Engineering College, Karachi
National University of Sciences and Technology, Islamabad, Pakistan

In partial fulfillment of requirements for the award of the degree of
MASTER OF SCIENCE IN ELECTRICAL ENGINEERING
Specialization in Communication
February 2015

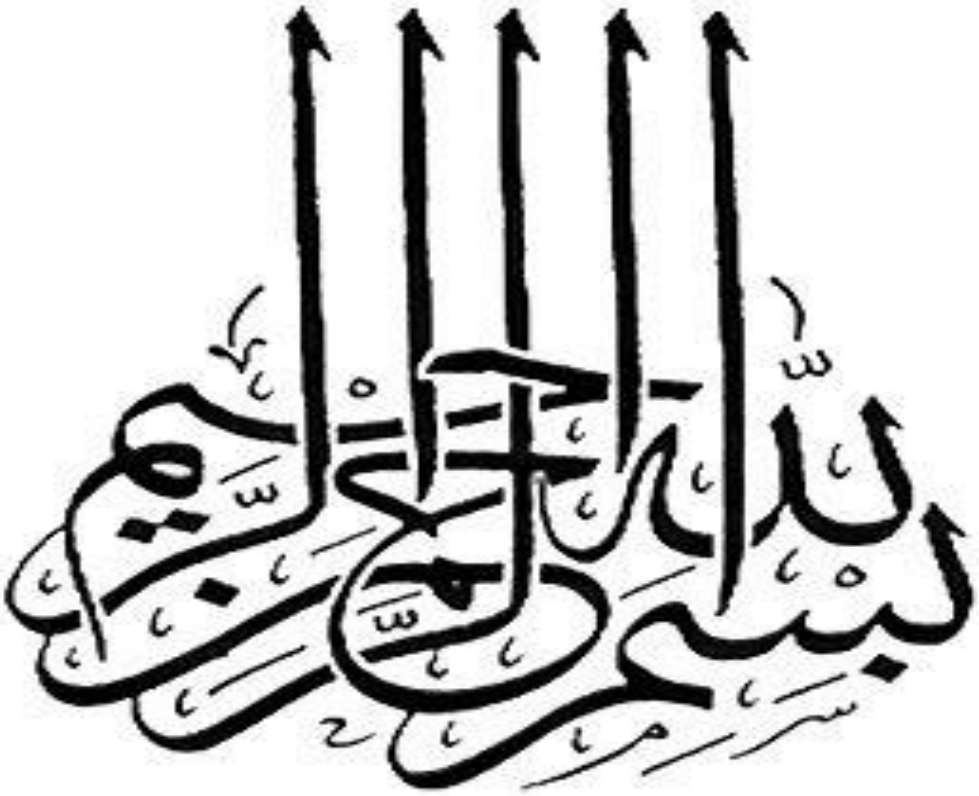
بسم الله الرحمن الرحيم

ACKNOWLEDGMENTS

All praise and thanks to the Almighty ALLAH (SWT) whom we seek help and guidance for sustenance. I am greatly indebted to my thesis supervisor Dr. Khawaja Bilal Ahmed Mahmood for his immense guidance, suggestions and wise reproach throughout the course of thesis. It is his insight and wide knowledge that guided me to the completion of this thesis work. Due to his broad research interests, he gave me the opportunity to explore many interesting antennas. He not only guided me but also assisted in practical matters. I express my sincere appreciation for his support. I would also like to express my gratefulness to the Head of the Department (PGS) Cdr. Dr. Ataullah for guiding and helping me in getting the project funds and showing his interest and permitting me to visit SEECS-NUST to complete my hardware. It is also worthy to present my thanks to Head of the RIMMS lab, SEECS-NUST Dr. Munir Tarar for giving prioritized access to the necessary equipment to test my hardware. The fabrication of antennas was carried out at the SEECS-NUST and would not have been possible without its resources. I feel pleasure to thank my GEC committee members, colleagues and all those who have helped me in any way for making this research a success.

Last but not least, I shall always remain highly obliged to my parents for giving me immense strength not only to set high goals but also to achieve them. Without their support, I would never have gotten so far.

ABSTRACT

As commercial population becomes mobile and with the advent of bandwidth hungry applications such as large file transfers, high-definition (HD) video streaming and wireless display etc., a wireless end-users now demands more bandwidth. Also, the spectral congestion at lower microwave frequencies is an important issue for the current wireless networks. To serve any number of mission-critical applications across all industries, the next generation of high-speed broad-band wireless access systems are now standardized which are referred to as 5th generation (5G) wireless local area networks (WLANs). The 5G wireless systems are required to transmit data at the speed of 1Gbps or above. Because of their backward compatibility and continuous progression, current WLAN standards have proved to be a hugely successful technology. In order to increase the capabilities and data-rates of the currently deployed WLANs, the industry has released its successive amendments which were rectified ever since 802.11b. The recently proposed WLAN standard is referred to as IEEE 802.11ac that offers higher data-rate as compare to currently available WLAN standards and operates in 5GHz frequency band. The key developments in 802.11ac include; wide channel bandwidth i.e. 20-, 40-, and 80MHz are necessary to achieve and 160MHz bandwidth is optional for high-capacity systems. Other improvements are the use of 256-level quadrature amplitude modulation (QAM) scheme which helps in providing increased capacity by utilizing available bandwidth. The increment in spatial streams i.e. up to 8 in total and up to 4 per client and multi-user multiple-input multiple-output (MU-MIMO) and beam-forming to increase effective coverage while providing interoperability are the techniques which are employed in 802.11ac standard. In order to achieve high data-rates, the current and expected future growth leads to the requirement of MIMO enabled antenna systems. Therefore, MIMO antenna systems are required by all newly

introduced wireless standards. The aim of this research study is to propose a MIMO antenna array design that can operate at 5GHz WLAN band and facilitates the features that conform to 802.11ac standard requirements. The proposed antenna array consists of eight radiating elements and is designed on two different software platforms i.e. Agilent advanced design system (ADS) and CST microwave studio that are based on different techniques. The comparative analysis of the antenna simulation results using both the techniques is presented. The antenna arrays are designed on a high i.e. Rogers RT/duroid 6010.2LM and a low end substrate i.e. FR-4; performance is evaluated for both substrates.

TABLE OF CONTENTS

LIST OF FIGURES

List of Tables

PUBLICATIONS

ISI Indexed Journal Papers

1. Asghar A. Razzaqi, Bilal A. Khawaja, Mehrab Ramzan, Javed Zafar, **Syeda Areeba Nasir**, M. Mustaqim, M. A. Tarar and T. Tauqeer, "A Triple-Band Antenna Array for Next-Generation Wireless and Satellite-Based Applications", accepted and published in *Cambridge International Journal of Microwave and Wireless Technologies (IJMWT)*, Aug 2014

2. Syeda Areeba Nasir, Bilal A. Khawaja, M. A. Tarar, T. Tauqeer and M. Mustaqim, "A 8-Element MIMO Antenna Array for Next-Generation 802.11ac Wi-Fi Applications", *Wiley Microwave and Optical Technology Letters*, Feb 2015 (In Submission)

Refereed Conference Papers

1. **Syeda Areeba Nasir**.; M. Mustaqim, ; B.A. Khawaja,, "Antenna array for 5th Generation 802.11ac Wi-Fi Applications", *High-capacity Optical Networks and enabling/Emerging Technologies (HONET-PfE 2014)*, 15-17 Dec, 2014, Charlotte, NC, USA *(Accepted for publication and addition in IEEE Xplore – Dec 2014)*

2. **Syeda Areeba Nasir**.; Arif, S.; Mustaqim, M.; B.A. Khawaja, "A log-periodic microstrip patch antenna design for dual band operation in next generation Wireless LAN applications," *Emerging Technologies (ICET), 2013 IEEE 9th International Conference on* , vol., no., pp.1,5, 9-10 Dec. 2013

3. Arif, S.; **Syeda Areeba Nasir**.; Mustaqim, M.; B.A. Khawaja, "Dual U-slot triple band microstrip patch antenna for next generation wireless networks," *Emerging Technologies (ICET), 2013 IEEE 9th International Conference on* , vol., no., pp.1,6, 9-10 Dec. 2013

Other Papers

1. Ali, S.H.; **Syeda Areeba Nasir**.; Qazi, S., "Impact of router buffer size on TCP/UDP performance," *Computer,Control & Communication (IC4), 2013 3rd International Conference on* , vol., no., pp.1,6, 25-26 Sept. 2013

CHAPTER 1: INTRODUCTION

1.1. Problem statement

1.1.1. General Background

As commercial population becomes mobile and with the advent of bandwidth hungry applications such as large file transfers, high definition video streaming and wireless display etc., a wireless end-users now demands more bandwidth. Also, the spectral congestion at lower microwave frequencies is an important issue for the current wireless networks. To serve any number of mission-critical applications across all industries, the next generation of high-speed broad-band wireless access systems are now standardized which are referred to as 5th generation (5G) wireless local area networks (WLANs) [1]. The 5G wireless systems are required to transmit data at the speed of 1Gbps or above [2]. Because of their backward compatibility and continuous progression, current WLAN standards have proved to be a hugely successful technology. In order to increase the capabilities and data-rates of the currently deployed WLANs, the industry has released its successive amendments which were rectified ever since 802.11b. The recently proposed WLAN standard is referred to as IEEE 802.11ac that offers higher data-rate as compare to currently available WLAN standards and operates in 5GHz frequency band. The 802.11ac standards fueled the industries with factors that include additional users, more devices per user “Bring Your Own Device” (BYOD), “Big” apps, cellular offloads etc [1].

1.1.2. Objective of the Study

IEEE identified a number of applications that require gigabit throughput. This serves as the basis for the 802.11ac development. The purpose of the research is to propose the design of an antenna system for next generation IEEE 802.11ac Wi-Fi application where IEEE 802.11ac is an emerging WLAN standard which uses 5GHz band. To meet the recent functional demands and the extensive wireless market growth expected in next 3-5 years are the real challenges for 802.11ac. The aim of this research is to propose an antenna design that can operate at 5GHz WLAN band and facilitates the features that conform to 802.11ac Wi-Fi standard. The increment in spatial streams i.e. up to 8 in total and up to 4 per client and multi-user multiple-input multiple-output (MU-MIMO) and beam-forming to increase effective coverage while providing interoperability are the techniques which are employed in 802.11ac standard [2-3].

1.2. MIMO

In order to achieve high data-rates, the current and expected future growth leads to the requirement of MIMO enabled antenna systems [4-6]. Although, designing a MIMO antenna system itself has unique challenges because modern wireless devices like laptops and tablets requires small-size antennas as there is much acute space available due to their compact sizes [7].

Multiple Input Multiple Output, or MIMO, is a form of smart antenna technology in which multiple antennas are used at both the transmitter and receiver ends to improve the data rate of a communication system. One of the main advantages of MIMO technology is that it increases data throughput and link range at a significant level without any increase in the channel bandwidth or transmit power [8]. The same total transmit power is spread over each of the antennas, which improves the spectral efficiency. Hence, providing more number of bits/sec/Hz

of the bandwidth [8]. The gain of each of the antenna element in the array is combined to form an array gain, which is much higher than a single element antenna. Because of all these interesting properties, the MIMO antenna systems are required by all newly introduced wireless standards.

The generic form of MIMO antenna system is shown in Fig. 1.1 (a). The transmitter is shown by *Tx* and the receiver is shown by *Rx*. It can be seen that multiple antennas are used at both the ends. Theoretically, the link throughput efficiency of a MIMO system is directly proportional with the number of antennas, *n*. The main concept behind the operation of MIMO is spatial multiplexing (SM) [6]. The SM is a transmission technique in which encoded data signals (also known as streams) can be transmitted separately and independently via each of the multiple transmit antennas. The space dimension is multiplexed more than one time. For example, if there are N_t antennas equipped on the transmitter and N_r on the receiver, the maximum number of streams (spatial multiplexing order) that can be generated is:

$$Ns = min\ (N_t, N_r) \tag{1.1}$$

It means that, ideally, a total of *Ns* independent parallel data streams can be transmitted simultaneously. This implies an *Ns* increase in spatial efficiency. The detailed MIMO transmission is depicted in Fig. 1.1 (b). The N_t antennas at transmitter, *Tx*, are sending data streams. There are N_tN_r transmission paths between N_t transmit antennas and N_r receiving antennas. Each of the receive antennas, N_r, receives a copy of N_t transmitted streams. The receiver gets the signal in the form of a vectors and and converts them into original information [6].

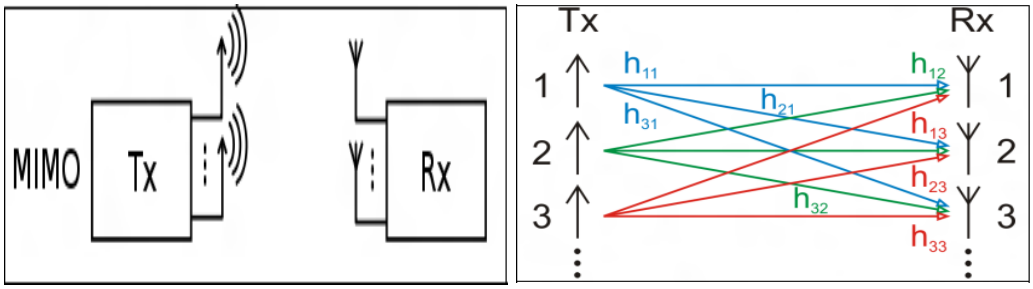

(a) (b)

Figure 1. 1: (a) General form of MIMO antenna system (b) Detailed depiction of MIMO transmission [8]

1.3. IEEE 802.11ac: The 5th Generation of Wi-Fi.

The 802.11ac standard is the most recent version of IEEE WLAN standards and uses MIMO technique plus 5GHz of unlicensed band speed up the data communication to a significant amount while making sure that the interference must be reduced as compared to 2.4GHz WLAN band. As shown in Fig. 1.2. IEEE 802.11ac offers higher data-rate as compare to currently available WLAN standards [1, 9].

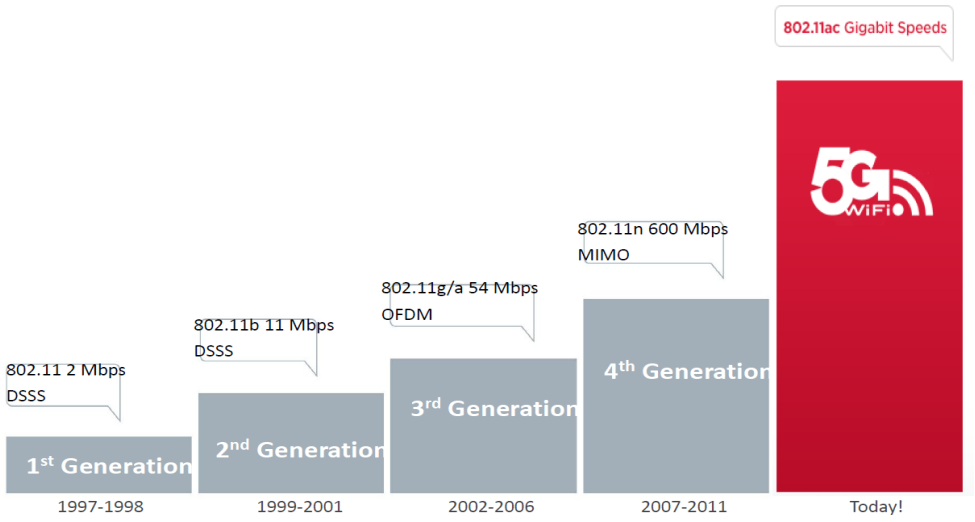

Figure 1. 2: IEEE 802.11ac: The 5th Generation of Wi-Fi [63]

The key developments in 802.11ac are depicted in Fig. 1.3. which include; wide channel bandwidth i.e. 20-, 40-, and 80MHz are necessary to achieve and 160MHz bandwidth is optional for high-capacity systems [1, 9]. Other improvements are the use of 256-level quadrature amplitude modulation (QAM) scheme which helps in providing increased capacity by utilizing available bandwidth [2-10]. The increment in spatial streams i.e. up to 8 in total and up to 4 per client and multi user multiple-input multiple-output (MU-MIMO) and beam-forming to increase effective coverage while providing interoperability are the techniques which are employed in 802.11ac standard [3].

Operation frequency	5-GHz unlicensed band only
Bandwidth	20, 40, and 80 MHz 160 and 80+80 MHz (optional)
Modulation schemes	BPSK, QPSK, 16QAM, 64QAM 256QAM (optional)
Forward error correction coding	Convolutional or LDPC (optional) with a coding rate of 1/2, 2/3, 3/4, or 5/6
MIMO	Space time coding, single-user MIMO, multi-user MIMO (all optional)
Spatial streams	Up to eight (optional)
Beamforming	Respond to transmit beamforming sounding (optional)
Aggregated MPDU (A-MPDU)	1,048,575 octets (65,535 octets in 802.11n)
Guard interval	Normal guard interval Short guard interval (optional)

Figure 1. 3: Key features of 802.11ac [11]

1.4. Thesis Approach

Until now IEEE 802.11ac has not been deployed in Pakistan and this is one of the initial efforts to design antennas that facilitate the features which conform to 802.11ac Wi-Fi standard. There is a need to develop cost effective antennas according to the recent functional demands.

The goal of this thesis is to develop a cost effective 8-Element MIMO antenna system that can support the features defined by IEEE 802.11ac: The 5th Generation of Wi-Fi. It will be

an indigenously designed MIMO antenna system. The proposed antenna will provide a solution for the antennas for 5G mobile communication systems.

Initially, the different types of patch antennas were simulated using Agilent's ADS software. The purpose behind the study was to select an antenna design that should provide an optimum solution for our approach. There are several different types of planar antennas available but in this design rectangular microstrip patch antenna (MPA) is selected because of its small size, light weight, low cost, good performance and installation ease. After the antenna design, simulations and optimization are completed the antennas will be fabricated and characterized. To achieve high accuracy, the antennas are fabricated by a commercial fabricator and the testing facility available at RIMS, SEECS-NUST is used for measurements and antenna characterization.

The following tasks are included in the Research/Thesis work:

- Literature study
- Antenna Designing
- Comparative study of the simulation results by using two different techniques i.e. FDTD and MoM
- Comparative study of the simulation results when antenna is designed on a high and a low dielectric substrate i.e. FR4 and Rogers 6010.2LM
- Development of prototypes on two different substrates i.e. FR4 and Rogers 6010.2LM
- Testing and verification
- Comparative analysis of measured and simulated results

1.5. Thesis Organization

The study comprises the following sections:

- Chapter 1 is an introductory chapter presenting the background of this study, main goals and purpose of the study.
- Chapter 2 is a relevant literature review in the study area, highlighting the previous research carried out in this domain.
- Chapter 3 presents a detailed introduction, operation and design procedure of microstrip patch antennas.
- Chapter 4 comprises of design methodology of 8-element MIMO antenna system
- In Chapter 5 measured and simulated results are discussed and comparisons that were carried out for different simulation techniques and substrates are presented.
- Finally, design and simulation results are concluded in Chapter 6.

CHAPTER 2: LITERATURE REVIEW

This chapter presents the significant research that has been carried out in the past, in an attempt to understand the basic and fundamental concepts of antenna. Evolution of the IEEE standards with in-depth discussion about IEEE 802.11ac is presented in this chapter.

2.1. Antenna Fundamentals

2.1.1. History of Antenna

Communications by electrical methods did not begin until the introduction of telegraphy in 1844, followed by the telephone in 1878. In these systems, the signals power is sent on two wire lines. Although Maxwell predicted theoretically in 1864 the existence of electromagnetic waves, they were not detected experimentally until Hertz in 1886 built a resonant radiating source at 75 MHz which consists of two coplanar flat metallic plates that are connected to an inductive coil and separated by a very precise gap over which sparks could propel quickly whereas the receiver system was formed by an open loop with a small gap over which sparks flow ensures unequivocal power transmission between both circuits. Hertz also built more sophisticated antennas such as Dipole antennas. In 1897, Marconi patented a complete system of telegraphy wires and in 1901 made the first transatlantic radio signals transmission. The receiving antenna raised it to 200 meters above ground level using kites [7, 12-14].

During 2nd World War new microwave devices culminated for radar applications. The new frequencies and antennas quickly took to establish fixed radios. The next pulse is given from the 60s to now with deep space communications and satellite communications. Introduction of computers and the massive applications of numerical methods and techniques (method of

moments, finite difference time domain...) have also allowed the researchers to analyze and synthesize new antennas optimized for a variety of applications [7, 15].

2.1.2. Definition of Antenna

The "Institute of Electrical and Electronics Engineers" (IEEE) defines an antenna that part of a transmitter or receiver system specifically designed in order to radiate or receive electromagnetic waves (IEEE Std. 145-1983) [64].

Antenna's performance characteristics include:

- Antenna's ability to radiate or receive in a certain direction (directionality).
- The operating or resonant frequency.
- Power levels must endure.
- The efficiency of the antenna.

2.1.3. Working Principle of Antenna

To get the knowhow of antenna's functionality and how it radiates, it's important to understand the phenomenon of radiation occurrence. The radiations occur as a result of time-varying current or an acceleration (or deceleration) of charge. There will be no radiation if there is no flow of charges or current in the wire. The uniform movement of charges in a straight wire will not even aid to emit radiations. On the other hand, if a curved or bent wire is used to flow electric charges with uniform velocity will result in a pattern of radiation. Even if the specific no. of charges oscillates with time flow in a straight wire will produce radiation as explained by Balanis [7].

Referring to the Fig. 2.1 below explains the radiation phenomenon, where two conductor's transmission line is connected to the voltage source. Application of voltage results in electric field in the transmission line which is referred to as electric lines of forces as depicted in Fig. 2.1. This field is sinusoidal in nature. The bunching of the electric lines of force represents the magnitude of the electric field. These electric lines of forces force these steady charges to move on and flow, as due to the current flow magnetic field is generated finally.

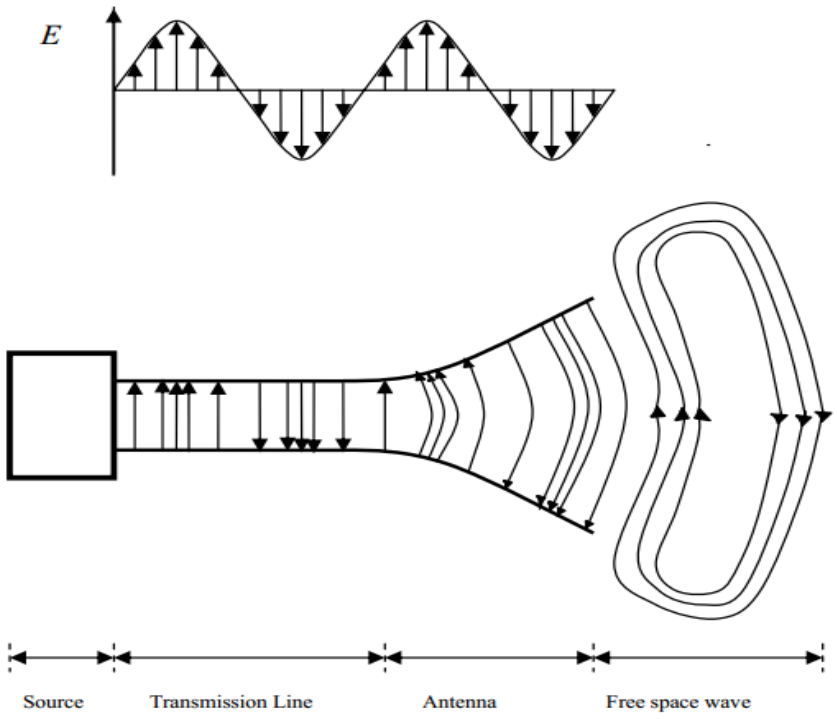

Figure 2. 1: Radiation from an antenna [13]

The created electromagnetic waves travel throughout the conductors as a result of these variant electric and magnetic fields. These continuously created waves as a result of continuous electric disturbance of sinusoidal source travel through transmission line, antenna and then to the free space. The electromagnetic waves are sustained inside the transmission line and antenna due

to the charges, but they form closed loops and are radiated as soon as they enter the free space [7].

2.1.4. Near and far field regions

The near field and far field are the regions of varying electromagnetic field around an antenna. The field regions define how the properties of an electromagnetic field change with respect to the distance from the source. The field patterns are related with two different types of energies; radiating energy and reacting energy. The surrounding space is divided into three regions as shown in Fig. 2.2 below.

- Reactive near-field region: This region is dominated by the reactive field. The field in this region appears as reactance because it oscillates towards and away from antenna. energy is stored in this region and does not dissipate. The distance of the outermost boundary for this region is given by $R1 = 0.62\sqrt{D^3/\lambda}$, where R1 is distance of the field boundary from the surface of antenna, *D* is the maximum dimension of antenna and λ is the wavelength of electromagnetic field.

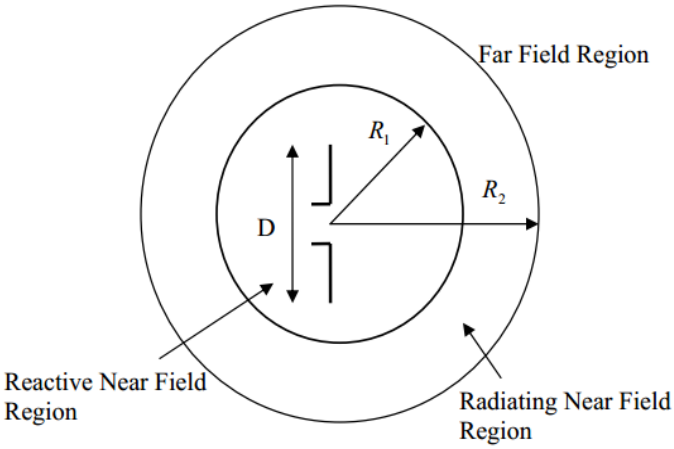

Figure 2. 2: Antenna Field Regions [13]

- Radiating near-field region: The radiating near-field region is also known as Fresnel region [6, 16]. It lies between the reactive near-field region and far field region. The reactive fields are smaller in region than in reactive near-field region. This region is dominated by the radiating fields. The distribution of the angular field in this region is a function of distance from the antenna. The range of the outermost boundary for this region is given by $R2 = 2D^3/\lambda$, where R2 is the distance of field boundary from surface of the antenna.
- Far field: The far field region is also known as Fraunhofer region [6, 16]. There are no reactive fields in this region. In the region far away from charge separations and currents, the electromagnetic field is affected by the charge in other fields and it is no longer affected by charge and current at source. The distant part of electromagnetic field becomes radiative field (also called far-field). Contrary to previous field types, the angular field distribution is independent of the distance from antenna in far-field region. The region beyond $R2 = 2D^3/\lambda$ is considered as far-field region.
- The differences between near and far field are shown quantitatively in Table 1:

Table 1: Near-Far field comparison [14]

Factors	**Near field**	**Far-field**
Carriers of the force	"Virtual photon"	Photon
Energy	Saves energy	Energy spreads via radiation field in space

Duration	Disappears when source is switched off	Radiation field is propagated, regardless of source, until it is absorbed
Interaction	The measurement or extraction of performance caused in the change in power source in the form of voltage or current changes	The measurement absorbs part of the radiation field, without affecting the source.
Field shape	Determined by the source and the geometry	Spherical waves that take against infinite distance planer shape.
Wave impedance	Depends on the source and medium	Depends only on the medium. In free space $120 \cdot \pi = 377\ \Omega$
Leadership	Energy can be selectively transferred via electrical lines	Energy can be in the form of waveguides are transported specifically

2.1.5. Reciprocity

Reciprocity is observed if cause can be interchanged, without changing the characteristic ratios. The electrical characteristics of an antenna for transmission and reception are identical and also radiation patterns are common for transmission and reception both. The conductor of

which the antenna is made should have same response to an electric field or current in one direction as it has to an electric field or current in another direction. Because of this property no distinction is made between transmitting and reception properties of an antenna. Same antenna can be used for transmission as well as reception [6, 18]. Optimized receiving antennas with amplifiers are generally adapted as otherwise transmit antennas [17, 18].

2.1.6. Antenna Parameters

The antennas are characterized by a number of parameters, the most common being listed below:

1. Radiation pattern

The radiation pattern is a graphical representation of the radiation characteristics of an antenna according to the direction (azimuth and elevation coordinates). The radiation properties which are considered for the radiation pattern include radiation intensity, flux density, field strength, phase, polarization and directivity. Considering the radiation pattern, antennas can be generally classified in different types and also it defines their directivity [14, 16, 18]. An isotropic antenna is a theoretical concept which radiates equally in all the directions. The radiation pattern of an isotropic antenna would look like a sphere. If power *P* is emitted by an isotropic antenna in a region of radius r, the power density *S* is given as [14]:

$$S = \frac{P}{area} = \frac{P}{4\pi r^2} \tag{2.1}$$

The radiation intensity for isotropic antenna U_i is given as [14]:

$$U_i = \frac{P}{r^2 S} = \frac{P}{4\pi} \tag{2.2}$$

It is impossible to design an isotropic antenna but there are some approximations of it known as omnidirectional antennas. The radiation pattern of an omnidirectional antenna, when

plotted, looks like a donut. The general form of radiation pattern of many antennas is shown in Fig. 2.3. The portion where most of the radiated power lies is known as “maxima” or “main lobe. Nulls are the portions where no power lies. Side lobes are smaller lobes which are separated but nulls. The back lobe or opposite lobe lies behind the main lobe. The most important parameters of the radiation pattern are:

- **Pointing direction:** The maximum radiation. Directivity and Gain.
- **Main lobe:** The angular range around the direction of maximum radiation.
- **Side lobes:** Side lobes are other relative maxima, lower the principal value.
- **Beamwidth:** The angular range of directions in which the radiation of a beam takes a value 3 dB below the maximum. That is, the direction in which the radiated power is halved.
- **Value of a secondary main lobe (SLL):** The ratio in dB between the maximum value of the main lobe and the maximum value of the secondary lobe.
- **Front-back ratio (FBR)** is the ratio in dB between the value of maximum radiation and the same direction and opposite direction [7, 14-16, 18].

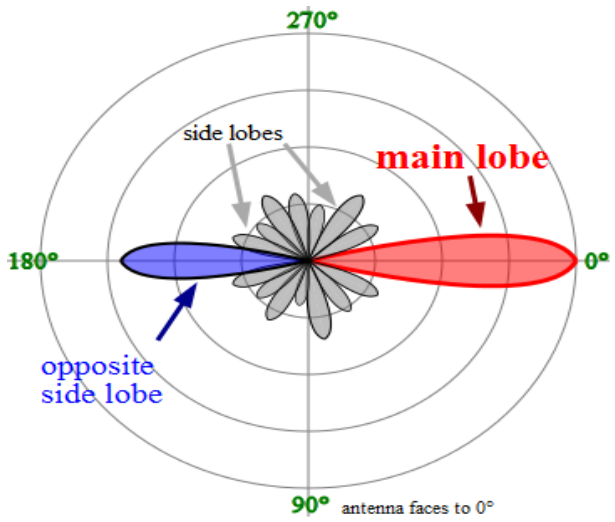

Figure 2. 3: General form of antenna radiation pattern [13]

2. Directivity

According to [7] the antenna directivity is defined as "the ratio of the radiation intensity in a given direction from the antenna to the radiation intensity averaged over all directions". In simple words, directivity of an antenna is the ratio of radiation intensity of an antenna to the radiation intensity of an isotropic antenna in a direction. Mathematical expression of directivity is given as

$$D = \frac{U}{U_i} = \frac{4\pi U}{P} \tag{2.3}$$

where D is the antenna directivity;

U_o is the radiation intensity of the antenna;

U_i is the radiation intensity of the isotropic antenna; and

P is the power radiated by the antenna.

In cases where the direction of the directivity is not indicated, the direction of maximum radiation intensity is implied. The maximum directivity is expressed as

$$D_{max} = \frac{U_{max}}{U_i} = \frac{4\pi U_{max}}{P} \tag{2.4}$$

Where D_{max} is the maximum directivity and

U_{max} is the maximum radiation intensity

Since the directivity is a ratio, it is a dimensionless quantity. It is expressed in dBi. The "i" refers to isotropic antenna. Narrower the front lobe of an antenna, greater is the directivity and vice versa. For a given polarization, the partial directivity is the part of radiation intensity in that polarization, divided by total radiation intensity averaged over all directions.

3. Gain

The gain of an antenna is closely related to its directivity. It measures the degree of directivity of an antenna's radiation pattern. Gain is defined gain as "the ratio of the intensity in a given direction, to the radiation intensity that would result if the power fed to the antenna were radiated isotropically" [15]. A high gain antenna will radiate more in a specific direction. A high gain antenna will provide increased range and better signal quality than isotropic antenna in a particular direction.

When referenced with an isotropical antenna, the antenna gain is given in dBi. Mathematically, gain is expressed as

$$D(\theta,\emptyset) = 4\pi \frac{radiation\ intensity}{toral\ input\ power} = 4\pi \frac{U(\Theta,\ \emptyset)}{P_i} \tag{2.5}$$

where $D(\Theta,\emptyset)$ is the directivity gain of the antenna;

$U(\Theta,\emptyset)$ is the radiation intensity of the antenna;

Θ and $\emptyset$ are the standard spherical coordinate angles; and

P_i is the total power radiated by the antenna. [6-7]

4. Return Loss (RL)

The return loss characterizes the relation between the input and output in a transmission line, especially when the load is mismatched and not all power is delivered to the load (antenna). For mismatched loads, some fraction of delivered power is reflected back to the source. The return loss shows the amount of power that is lost to the load and does not return as reflection. The return loss is given by:

$$RL = -20\log|\Gamma| \quad \text{(dB)} \tag{2.6}$$

where

$$|\Gamma| = \frac{V_0}{V_{in}} = \frac{Z_L - Z_0}{Z_L + Z_0} \tag{2.7}$$

$|\Gamma|$ = magnitude of reflection coefficient

V_o = reflected voltage

V_{in} = input voltage

Z_L and Z_o are the load and characteristic impedances.

For the case of perfect matching when no power is reflected back, Γ=0 and RL= -∞. Whereas, Γ=1 and RL= 0 imply that all of the transmitted power is reflected back to the source. For practical applications, an RL of -10 dB or below is considered as acceptable which is directed to the fact that reflected signal is less than 10% of what was transmitted.

5. Input Impedance

The antenna input impedance is defined as "the impedance presented by an antenna at its terminals or the ratio of voltage to current at pairs of terminals" [7]. It can also be considered as the ratio of electric field to magnetic field at a point. Mathematically, input impedance is written as:

$$Z_{in} = R_{in} + jX_{in} \tag{2.8}$$

where Z_{in} is the antenna impedance

R_{in} is the antenna resistance

X_{in} is the antenna reactance

R_{in} is composed of two parts, radiation resistance R_r and loss resistance R_L. The power that is acutally radiated by antenna is related with R_r and the power which is dissipated as heat or other losses is related with R_L. The imaginary part, X_{in}, is related to the power stored in near field of the antenna.

6. Antenna Efficiency

The parameter of antenna efficiency considers the amount of losses at antenna terminals and physical structure of antenna. These losses may include:

- Reflections due to mismatch between the transmitter and receiver
- I^2R (power losses)

So, overall efficiency is given by:

$$e_t = e_r\, e_c\, e_d \tag{2.9}$$

where e_t = total efficiency

e_r = reflection efficiency = $(1 - |\Gamma^2|)$

e_c = conduction efficiency

e_{ss} = dielectric efficiency

7. Polarization

Polarization is a parameter which tells about the orientation of the electric field of an electromagnetic wave in far-field region. In [7] it is defined as "the property of an electromagnetic wave describing the time varying direction and relative magnitude of the electric field vector". The position and direction of electric field wave is taken with reference to the earth's surface to determine its polarization. When direction of antenna radiation is not stated, the polarization is taken in the direction of maximum gain [6]. Some common types of polarization include linear, circular, elliptical, circular left hand, circular right hand, elliptical left hand and elliptical right hand polarization.

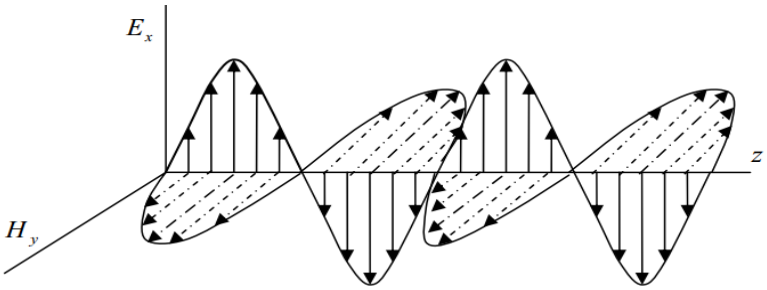

Figure 2. 4: Linearly polarized electromagnetic wave [7]

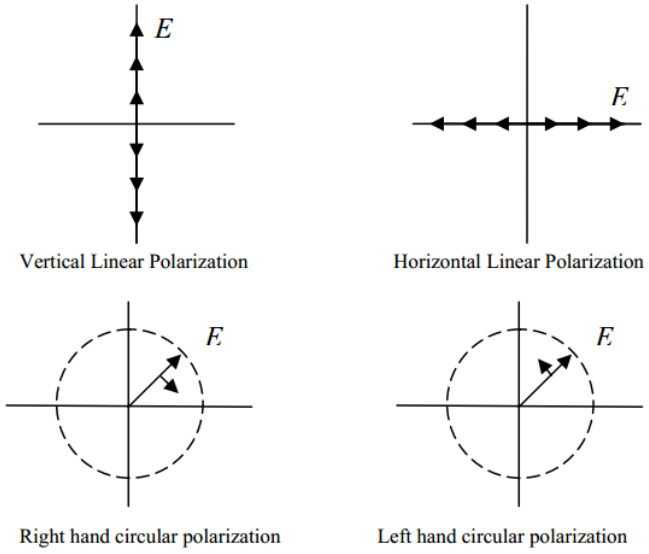

Figure 2. 5: Linear and circular polarizations [13]

Fig. 2.4 shows a linearly polarized wave. In linear polarization, the path of electric field vector is back and forth along a straight line. Whereas in circular polarization, the magnitude of the electric field vector remains constant but it rotates around a circular path. When the vector routes counterclockwise it is called left hand circular polarization and when it rotates clockwise it is called right hand circular polarization, as shown in Fig. 2.5.

8. Voltage Standing Wave Ration (VSWR)

Maximum power transfer from the transmitter to the antenna should take place in order for antenna to operate efficiently. This can only take place if the input impedance of antenna, Z_{in}, matches with impedance of source or transmitter, Z_S. The power transfer theorem states that "only if impedance of the transmitter is a complex conjugate of the impedance of the antenna, the maximum power can be transferred, or vice versa". This condition is written mathematically as:

$$Z_{in} = Z_S \tag{2.10}$$

where $Z_{in} = R_{in} + jX_{in}$

$Z_S = R_S + jX_S$

When this condition is not met, some of the power reflects back to the source and which, in turn, create standing waves in transmission line. These standing waves are characterized by a term known as voltage standing wave ratio (VSWR). VSWR is given by [18] as:

$$VSWR = \frac{1+|\Gamma|}{1-|\Gamma|} \tag{2.11}$$

where Γ is called reflection coefficient

Basically, VSWR is the measure of mismatch between transmitter and antenna. Lesser the value of VSWR, lower is the mismatch and vice versa. For a perfect match, the VSWR is unity.

9. Bandwidth

Antenna bandwidth is defined by [7] as "the range of frequencies for which the performance of antenna conforms to a specific standard". The bandwidth of an antenna can be thought as the range of frequencies on both sides of the counter frequency where the antenna

parameters are close to those obtained at center frequency. These antenna parameters include input impedance, radiation pattern, beamwidth, polarization or gain. Bandwidth of broadband and narrowband antenna is obtained by equations 2.12 and 2.13, respectively.

$$BW_{broadband} = \frac{f_H}{f_L} \tag{2.12}$$

$$BW_{narrowand}(\%) = \left[\frac{f_H - f_L}{f_C}\right] \times 100 \tag{2.13}$$

Where f_H = upper frequency

f_L = lower frequency

f_C = center frequency

For a broadband antenna, $\frac{f_H}{f_L} = 2$. Antenna performance in the required frequency band is measured by its VSWR in that band. A *VSWR ≤ 2* (*RL ≤ -10 dB*) ensures satisfactory performance. Fig. 2.6 shows how to measure antenna bandwidth from its return-loss plot.

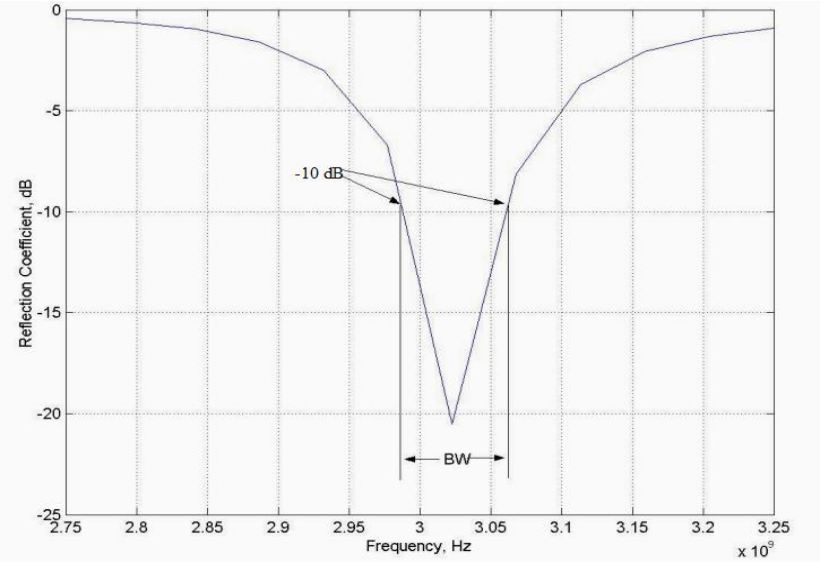

Figure 2. 6: Measuring antenna bandwidth from return loss plot [13]

10. Beam Efficiency

Beam efficiency is a parameter used to judge the quality of transmitting and receiving antennas. The beam efficiency B of an antenna having its major lobe directed along the z-axis (θ=0 degree) is given as:

$$B = \frac{Power\ transmitted\ (received)\ within\ cone\ angle\ \theta}{Power\ transmitted\ (received)\ by\ the\ antenna} \quad (2.14)$$

Where θ is the half angle of the antenna radiation cone.

11. Resonance frequency

Usually referred as operating frequency of an antenna and is defined as the frequency at which reactive components of the antenna cancels each other showing only resistive part because of having equal magnitudes but opposite phases. Under these conditions, the conversion of electrical energy into electromagnetic waves (or vice versa) is maximum. The resonance frequency of an antenna depends directly on the size of the active element, so that as the frequency increases decreases the size of the antenna [7].

2.1.7. Antenna Types

Depending upon their structure, characteristics and behaviors, there are various types of antenna. The most used and popular ones are discussed below:

2.1.7.1. Horn Antenna

A horn antenna [6-7] is a design of an antenna for microwave and consists of a more or less the shape of an exponential horn approximated metal surface, usually in a waveguide's ends. Horn are used as independent emitters or to feed at the focus of parabolic antennas (radar

antennas, radio telescopes, radio antennas, antennas mussel). Different models also led to names such as pyramidal horn and tapered horn etc [18].

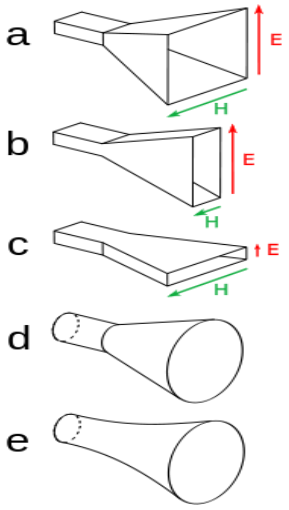

Figure 2. 7: Horn Antenna shapes: (a) the pyramid, (b) E-flat shape, (c) H-flat shape (D) conical, (e) exponentially [19]

In principle, the waveguide antenna that directs the transmitter power from its open end in the free space, the impedance transition causes some reflections of wave energy which is due to the fact that impedance of the vacuum has a value other than the waveguide. Therefore, changes were made to the mechanical dimensions of the waveguide at the point of exit of the electromagnetic wave radiation, to achieve a gradual transition. This construction is called because of the horn-like shape "horn". In microwave antennas, the combination of a primary radiator and a secondary reflector is common, where as a primary radiator at the focal point of a metallic parabolic mirror often a horn antenna (feed) is used [14, 16-18].

2.1.7.2. Loop Antenna

A loop antenna consists of a wire, tube or other metal bent into a closed circular or a rectangular shape with its ends (terminals) connected to a transmission line [15]. Loop antennas

are of two types: small loop antennas and large loop antennas, shown in Fig. 2.11. The loop circumference of a small loop antenna is much smaller as compared to wavelength ($L << \lambda$) [14, 16]. To ensure a constant current distribution across the loop, it should be of the length of $\lambda/10$ or less [18]. When the circumference of a loop antenna is approximately equal to the wavelength, it is said to be a large loop antenna.

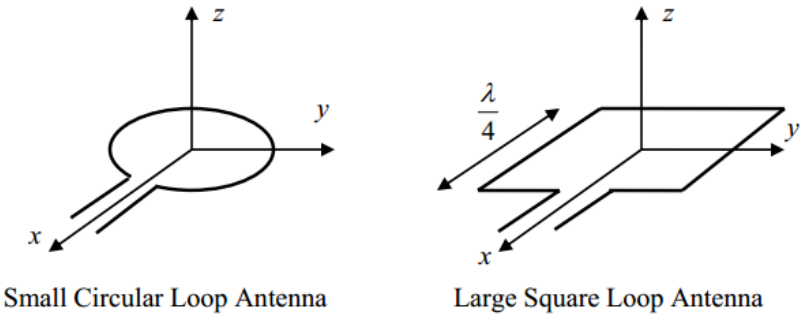

Figure 2. 8: Loop antennas [13]

Small loop antennas usually have poor efficiency and are mainly used for receivers at low frequencies. When the loop size is increased, the standing waves start to develop in current and antenna start to behave like large loop or self-resonant antenna. Filling loop core with ferrite helps increasing performance of a loop antenna because it increases the radiation resistance [6].

The loop antennas have a usual gain of 3dBi and bandwidth of 10% [14]. The large or self-resonant loop antenna of the length of one wavelength, compared to dipole, transmits less toward ground or sky. This property gives it a higher gain in horizontal direction. Large loop antenna radiates in the direction normal to the plane of loop. Polarization of such antenna is not known from its orientation; rather it depends upon the feed point. When it is fed from inside, the polarization becomes vertical and if fed at the bottom, it will be horizontally polarized. Better directivity can be achieved by increasing loop circumference up to 3 or 5 wavelengths. It can be

noticed from Fig. 2.9 that radiation patter of large loop antenna is different than that of small loop antenna.

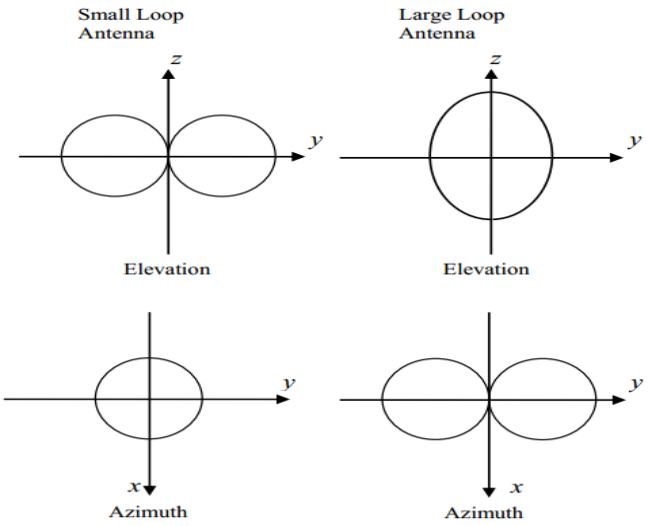

Figure 2. 9: Radiation patters of small loop and large loop antenna [13]

2.1.7.3. Helical Antenna

A helical antenna, also known as helix, is an antenna consisting of a conducting wire wound in the shape of a helix, mounted over a ground plane. The feed line is connected between ground and bottom of the helix. Fig. 2.10 shows a common helix antenna. The two principal modes of helical antennas are normal mode (broadside radiation) and axial mode (endfire radiation) [6].

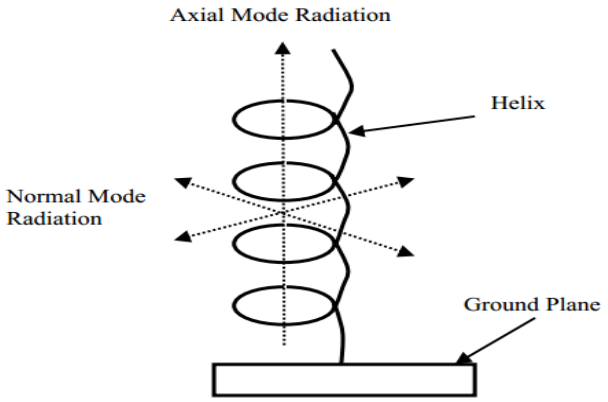

Figure 2. 10: Helical antenna [14]

The helical antenna operates in the normal mode when its dimensions are small as compared with the wavelength. In this mode, the antenna acts as a electrically short dipole or monopole and its radiation pattern is omnidirectional with maximum radiation in the direction of right angles to the helix axis and minimum in the direction of helix. The normal mode usually provides low bandwidth.

The helix operates in axial mode if its size is comparable to or above the wavelength. The antenna radiates a main directional beam along the axis of the helix. The waves in this mode are circularly polarized. The circular polarization is useful where the relative polarization of transmitting and receiving antenna is hard to maintain. The ground plane acts as a reflector which reflects the waves forward to make it directional such as in space communication. It provides gain of up to 15dBi and bandwidth ratio of 1.78:1 as compared to normal mode helix [12]. The antenna can be made more directional by increasing the number of turns. The radiation patter of both the modes is shown in Fig. 2.11.

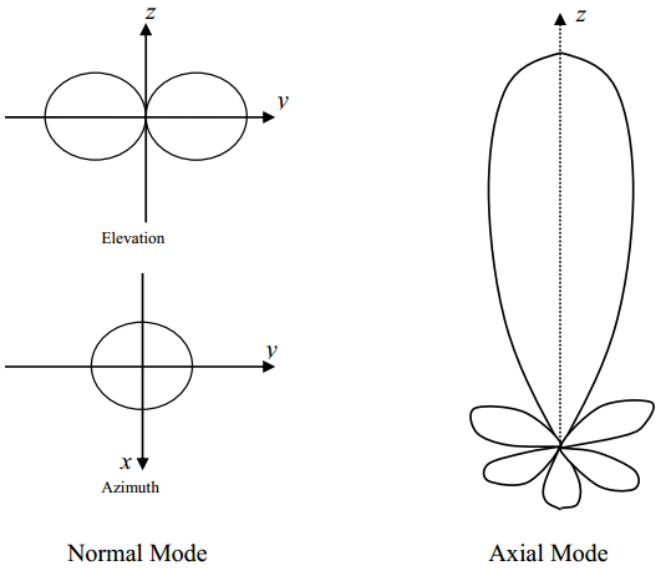

Figure 2. 11: Radiation pattern of normal and axial mode helical antenna [14]

2.1.7.4. Monopole Antenna

A monopole antenna consists of a straight rod-shaped conductor mounted perpendicularly over a conductor known as a ground plane. Fig. 2.12 shows a typical monopole antenna. The monopole antenna is formed by applying image theory to a dipole antenna which states that "if a conducting plane is placed below a rod-shaped metallic element carrying a current, an image of the conducting element is formed below the plane". The combination of the element and its image is identical to a dipole of length *λ/2*. The length of element is *λ/4*. In this case, the radiation only occurs above the ground plane [14].

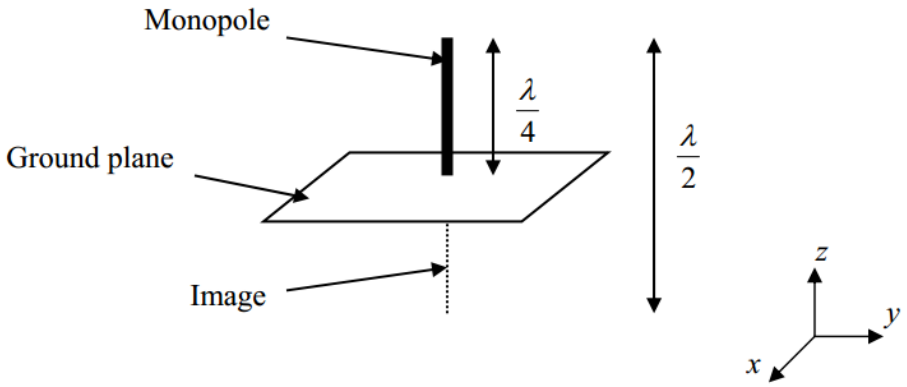

Figure 2. 12: Monopole antenna [14]

The quarter-wave monopole antenna is an approximation of half-wave dipole. As compared to a dipole, the directivity of a monopole antenna is doubled and radiation resistance is halved. The monopole antenna is very useful in the mobile applications because it is half the size of dipole antenna. While used on car, the body of car acts as ground plane. The gain of a quarter-wave monopole is 5.19 dBi and its radiation resistance is 36.8Ω [7, 14]. Electrically small ground plane is sometimes used to tilt the direction of maximum radiation. The radiation pattern of a monopole antenna is shown in Fig. 2.13.

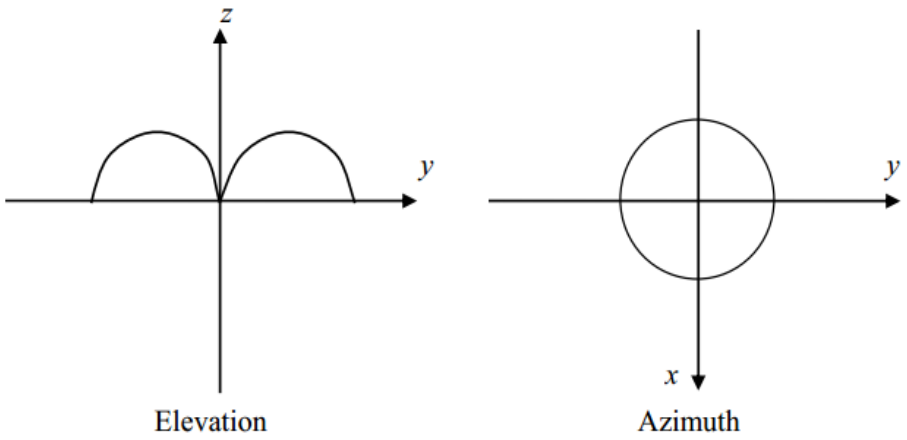

Figure 2. 13 Radiation pattern of monopole antenna [14]

2.1.7.5. Half-wave Dipole Antenna

A half-wave dipole antenna is made of two metal conductors of wire or rod arranged in line with each other, with a small space between them. One of the two elements is center-fed driven element. Each of these elements are of the length of quarter wavelength which makes total antenna length of half wavelength or λ/2, as shown in Fig. 2.14. Dipoles can be shorter or longer than λ/2 according to required antenna performance but half wavelength is widely used.

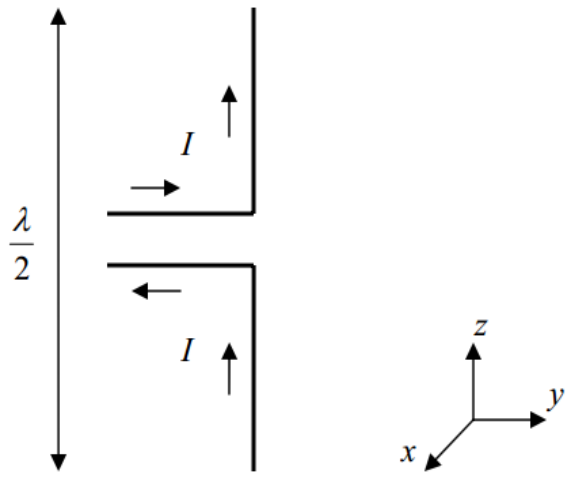

Figure 2. 14: Half wave dipole antenna [14]

As shown in Fig. 2.14, the dipole is fed by a two-wire transmission line. We can see that the current in both the wires is opposite in direction, but of sinusoidal distribution and equal amplitude. No radiation occurs in transmission line due to cancelling effect. Whereas, the current in the dipole flows in same direction and produce radiation. The vertical orientation of dipole produces horizontal radiation and horizontal orientation produces vertical radiation. A dipole antenna has a gain of about 2.15 dBi, bandwidth of 10% and radiation resistance of 73 Ω [12]. Radiation pattern of a half wave dipole antenna is shown in Fig. 2.15.

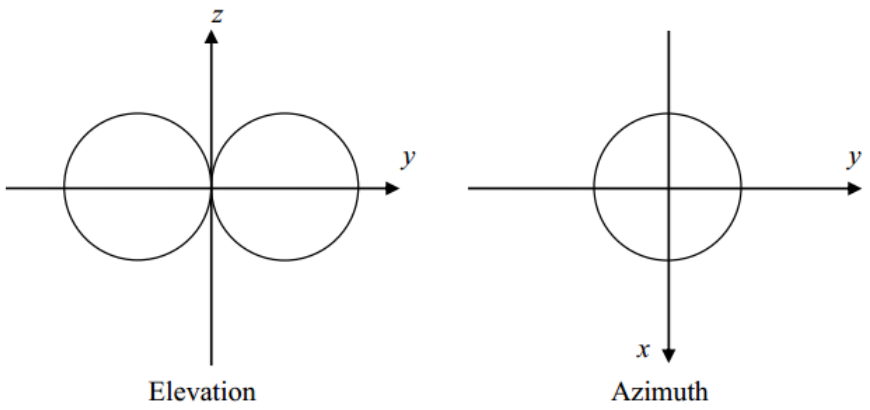

Figure 2. 15: Radiation pattern of a half wave dipole antenna [14]

2.2. IEEE 802.11 Standard and its Successive amendments

802.11 is a family of standards for wireless local area networks (WLAN). The definition of the IEEE 802 standards, the general first describe the network access, began in February 1980, hence the name was chosen 802 [2] [20-23].

802.11 has a variety of standards as shown in Table 2, each with a letter suffix. These cover everything from the wireless standards themselves, to standards for security aspects, quality of service etc.

Table 2: IEEE 802.11 Wi-Fi Standards [24]

IEEE 802.11 Standards	
802.11a	Wireless network bearer operating in the 5 GHz ISM band with data rate up to 54 Mbps
802.11b	Wireless network bearer operating in the 2.4 GHz ISM band with data rates up to 11 Mbps
802.11e	Quality of service and prioritization
802.11f	Handover
802.11g	Wireless network bearer operating in 2.4 GHz ISM band with data rates up to 54 Mbps
802.11h	Power control
802.11i	Authentication and encryption
802.11j	Interworking
802.11k	Measurement reporting
802.11n	Wireless network bearer operating in the 2.4 and 5 GHz ISM bands with data rates up to 600 Mbps
802.11s	Mesh networking
802.11ac	Wireless network bearer operating below 6GHz to provide data rates of at least 1Gbps per second for multi-station operation and 500 Mbps on a single link
802.11ad	Wireless network bearer providing very high throughput at frequencies up to 60GHz
802.11af	Wi-Fi in TV spectrum white spaces (often called White-Fi)

Among all the 802.11 Wi-Fi standards described, 802.11 a/b/g and n are commonly used standards of wireless network. All of these standards are developed in different times and have different features to offer according to the needs and necessities of that time. They operate within

the ISM (Industrial, Scientific and Medical) frequency bands. These are shared by number of other users, and no license of operation within these frequencies is needed [24].

The first introduced 802.11 WLAN standard was 802.11b. In order to increase the capabilities and data-rates of the currently deployed WLANs, the industry has released its successive amendments which were rectified ever since 802.11b. Key features of successive amendments of 802.11 standards are summarized in Table 3. The recently proposed WLAN standard is referred to as IEEE 802.11ac that offers higher data-rate as compare to currently available WLAN standards and operates in 5GHz frequency band [1, 9].

Table 3: Key features of IEEE 802.11 Wi-Fi Standard [25]

Standard	Year	Band	Bandwidth	Modulation	Antenna Technology	Data Rate
802.11b	1999	2.4 GHz	20 MHz	CCK	—	11 Mb/s
802.11a	1999	5 GHz	20 MHz	OFDM	—	54 Mb/s
802.11g	2003	2.4 GHz	20 MHz	CCK, OFDM	—	54 Mb/s
802.11n	2009	2.4 GHz, 5 GHz	20 MHz, 40 MHz	OFDM (up to 64-QAM)	MIMO with up to four spatial streams, beamforming	600 Mb/s
802.11ac	—	5 GHz	40 MHz, 80 MHz, 160 MHz	OFDM (up to 256-QAM)	MIMO, MU-MIMO with up to eight spatial streams, beamforming	6.93 Gb/s
802.11ad (WiGig)	—	2.4 GHz, 5 GHz, 60 GHz	2.16 GHz	SC/OFDM	Beamforming	6.76 Gb/s

2.2.1. IEEE 802.11ac

As the 5th generation of Wi-Fi standards (as a sequel of IEEE 802.11n), IEEE 802.11ac offers robust network, enhanced data rates, efficient RF bandwidth utilization and more over the course reliability [3]. The 802.11ac seems to be an evolution rather than revolution in stepping

up 802.11n, as it relies significantly on algorithms previously ironed out through the development of 802.11n [26].

2.2.1.2. Why 802.11ac is needed?

As commercial population becomes mobile and with the advent of bandwidth hungry applications such as large file transfers, high definition video streaming and wireless display etc., a wireless end-users now demands more bandwidth [9, 27]. Also, the spectral congestion at lower microwave frequencies is an important issue for the current wireless networks. To serve any number of mission-critical applications across all industries, the next generation of high-speed broad-band wireless access systems are now standardized which are referred to as 5th generation (5G) wireless local area networks (WLANs) [1-4]. The 5G wireless systems are required to transmit data at the speed of 1Gbps or above. Because of their backward compatibility and continuous progression, current WLAN standards have proved to be a hugely successful technology.

2.2.1.3. Key Developments of IEEE 802.11ac

The key developments in 802.11ac include; wide channel bandwidth i.e. 20-, 40-, and 80MHz are necessary to achieve and 160MHz bandwidth is optional for high-capacity systems [1, 9]. Other improvements are the use of 256-level quadrature amplitude modulation (QAM) scheme which helps in providing increased capacity by utilizing available bandwidth [2-10]. The increment in spatial streams i.e. up to 8 in total and up to 4 per client and as depicted in Fig. 2.16, multi user-multiple-input multiple-output (MU-MIMO) and beam-forming to increase effective

coverage while providing interoperability are the techniques which are employed in 802.11ac standard [3]. Key features of IEEE 802.11ac are precisely presented in Table 4 below.

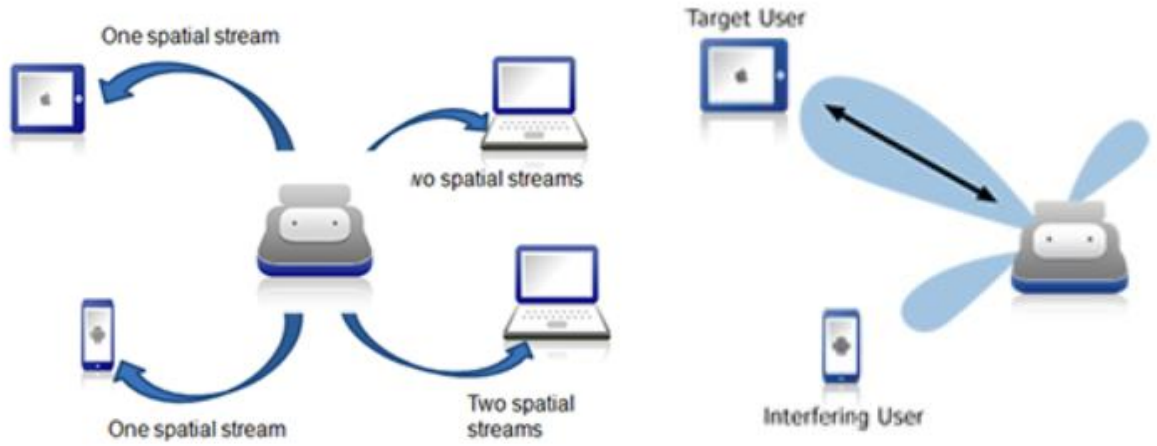

(a) (b)

Figure 2. 16: (a) MU-MIMO and (b) Beam-forming [3]

Table 4: Key features of IEEE 802.11ac Wi-Fi Standard [11]

Operation frequency	5-GHz unlicensed band only
Bandwidth	20, 40, and 80 MHz 160 and 80+80 MHz (optional)
Modulation schemes	BPSK, QPSK, 16QAM, 64QAM 256QAM (optional)
Forward error correction coding	Convolutional or LDPC (optional) with a coding rate of 1/2, 2/3, 3/4, or 5/6
MIMO	Space time coding, single-user MIMO, multi-user MIMO (all optional)
Spatial streams	Up to eight (optional)
Beamforming	Respond to transmit beamforming sounding (optional)
Aggregated MPDU (A-MPDU)	1,048,575 octets (65,535 octets in 802.11n)
Guard interval	Normal guard interval Short guard interval (optional)

2.2.1.4. 802.11ac VS 802.11n

The 802.11ac represents the 5th generation of IEEE 802.11 WLAN standards and is expected to deliver a data rate connection of at least three times that of 802.11n which is depicted in Fig. 2.17. Many of the algorithms of 802.11n are being reused, but enhanced, with 802.11ac, which should make the technology easy to fold into existing networks [26]. Existing 802.11 technologies operate in the 2.4 GHz band (802.11b, 802.11g), the 5 GHz band (802.11a), or both (802.11n). The 802.11ac operates strictly in the 5GHz band, but supports backwards compatibility with other 802.11 technologies operating in the same band (most notably 802.11n) [3]. A comparison of the characteristics of 802.11n vs. 802.11ac is shown in Table 5.

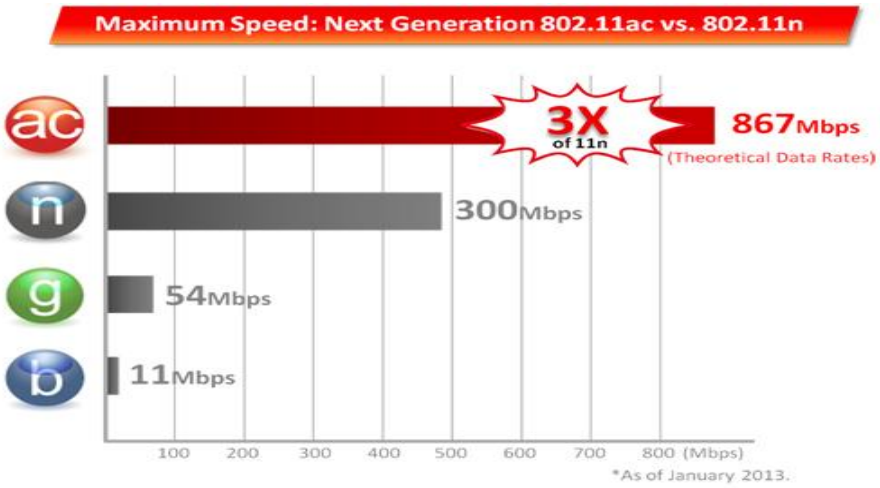

Figure 2. 17: 802.11ac Vs 802.11n [28]

Table 5: 802.11n VS 802.11ac [11]

802.11N VERSUS 802.11AC							
IEEE standard	Ratification date	Band	Technology	Modulation	Channel bandwidth	MIMO	Maximum speed
802.11n	2009	2.4 and 5 GHz	OFDM	Up to 64QAM	20, 40 MHz	Up to 4x4	600Mbits/s
802.11ac	Mid-2012 expected	5 GHz	OFDM	Up to 256QAM	40, 80, 160 MHz	Up to 8x8	3 Gbits/s+

2.3. Computational Electromagnetic Software

This section presents some very well known design techniques, particularly the CST Microwave Studio's implemented "Finite Difference Time Domain" (FDTD) technique and ADS momentum's implemented Method of Moments (MoM), the computational electromagnetic software used in this study. The target of this research is to design, test, and analyze the characteristics of an 8-Element MIMO antenna system for IEEE 802.11ac Wi-Fi application by using the CST Microwave Studio which is FDTD based software and ADS momentum that uses MoM so that performance can be evaluated for both.

2.3.1. Finite Difference Time Domain (FDTD) Method

In order to discretize Maxwell's equations, FDTD uses approximate differential operators. Finite differences help Maxwell's equation to discretize approximate differential operators that are applied in the FDTD method in this perspective. The real advantage FDTD technique posses is the arbitrary shapes' structural analysis and materials' large variety. Independent permittivity and permeability of per volumetric cell is one of the noteworthy features in this technique. Introducing the incident plane wave into the grid and transmitting it in discrete steps towards target is the manner in this approach. Without causing the introduction of artificial reflections, the scattered field must leave the grid.

At the grid boundary, the Perfectly Matched Layer (PML) boundary is normally used. In order to filter out the lately occurred residual reflections from the grid boundary, larger grids are also an option. Courant conditions should be complied, linking the spatial discretization (cell size) and the time steps (discrete) in order to get stability. As solutions at multiple frequencies are acquired through calculation of single time domain, FDTD is suitable for every broadband

excitation. In order to get the required parameters over a large bandwidth, fourier transform of the scattered waveforms (time-sampled) are used. For quick and perfect 3D electromagnetic simulations of high-frequency requirements, CST microwave studio is the best option. Using its fully parameterized magnetostatic and electrostatics solvers, CST provides some noteworthy features i.e. automatic macro recording, VBA compatibility, automatic multi-dimensional optimizers and parameter sweeps [29].

CST based modeling ensures inputting data via interactive mouse, capturing design, assisting templates for particular applications and also 3D modeling (fully parametric). Editing can be done in infinite terms as “undo” and “redo” options are available via “history list”. Helices, chamfers, blends, lofting, extrusions and boolean operations (i.e. adding and subtracting solid objects from existing structures) are some of the additional and advanced solid modeling features this software offers. It also supports importing 3D and planar structures and imported objects’ parameterization [29].

Automatic and refined meshing refinements are also some options this software offers. Either these materials are magnetic or non-magnetic, linear or non-linear, isotropic or anisotropic; they can be arranged in layers. Plane wave incident fields, waveguide ports, and discrete V and I sources are some of the included RF energy excitation sources. The post-processing comprises of port signal plots, polar radiation pattern plots, VSWR/smith chart plots, and 2D/3D field plots. Significantly important for antennas (circularly and elliptically polarized), this software also tends to plot and calculate axial ratio of an antenna [29].

2.3.2. Method of Moments (MoM)

The other simulation method examined in this study is Method of Moments which is implemented in ADS-Momentum. Usually referred as (3D planar solver), MoM simulation method is among one of the most tricky to implement methods of EM simulation because of its careful assessment of Green's functions and coupling integrals [30]. The MoM technique posses a major practical advantage i.e. its only required in the structure being simulated to discretize (mesh) the metal interconnects despite the reason that the distribution of current on the surfaces of metal are still core unknowns. This can be presented as alternate to those techniques where electric/magnetic fields (present ubiquitously in the solution space) are as the core unknowns.

The simplicity and easy implementation of 'planar' MoM mesh over equivalent '3D volume' mesh essential for FEM/FDTD simulation is the reason of it. An efficient MoM mesh will be conformal (mesh cells are only created on the metal interconnects) and will typically consist of rectangles, triangles and quadrilateral shaped mesh cells. A reduced number of mesh cells lead to fewer unknowns and an extremely efficient simulation. This makes MoM well suited for the analysis of complex (layered) structures. Another benefit of the MoM technique is that only one matrix solve is required for all port excitations, in other words there is no significant time penalty associated with simulating designs requiring a large numbers of ports [31].

To balance the efficiency benefits of the MoM technique we also have to consider some of the potential limitations and it is important to recognize that the MoM technique is not applicable for general 3-dimensional structures. As already stated that the MoM technique relies upon the computation of Greens functions which are only available for free space or for structures that fit in a layered stack up. This in-turn means that the structures being simulated

must be ‘planar’ in nature and fit within the layered stack up (drawn in the x-y plane) or be planar objects (drawn in the x-y plane) which are extruded vertically (along the z-axis) through the layered stack up. Fortunately, for many RF/Microwave technologies this limitation is not significant because the technology is often planar in nature. Think of a multi-layer PCB or a MMIC structure, this typically consists of a layered stack up (substrate dielectric layers) and interconnects (metal traces). The interconnects are printed in the x-y plane at various interface locations in the substrate and via contacts between metal layers can be considered 2D objects (cross sections) extruded vertically through the substrate layers [31].

CHAPTER 3: MICROSTRIP PATCH ANTENNA

In recent decades there has been an emerging high technology development in various media and therefore the world of telecommunications, with a strong tendency in search of miniaturization and in turn high performance equipment designed for purposes. For example, one might consider about high performance telecommunications requirements of the aerospace company, in spacecraft, the various applications in satellites and missiles; where size, weight, cost, performance, ease of installation and aerodynamic contour are important parameters when choosing the different devices for communications which includes antennas as well. And it is in these environments where low profile antennas such as microstrip patch antennas, may be required [32, 33].

3.1. What is Microstrip Patch Antenna?

A microstrip patch antenna (MPA) consists of a radiating patch on one side and a dielectric substrate which has a ground plane on the other side as shown in Fig. 3.1. The patch is generally made of conducting material such as copper or gold and can take any possible shape (see Fig. 3.2).

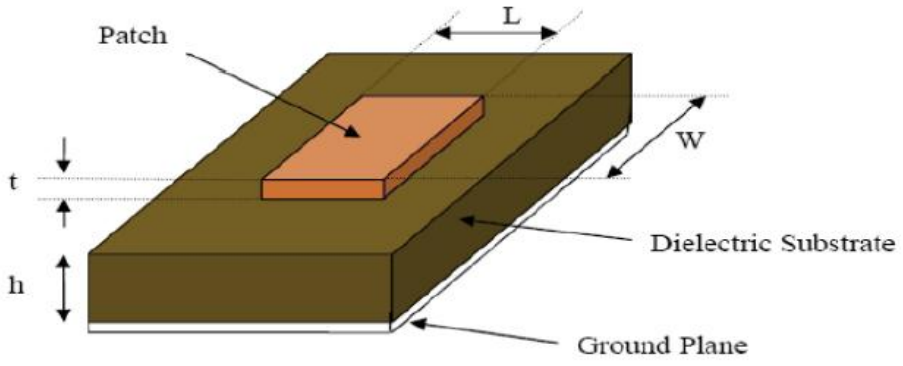

Figure 3.1: A Microstrip Patch Antenna [43]

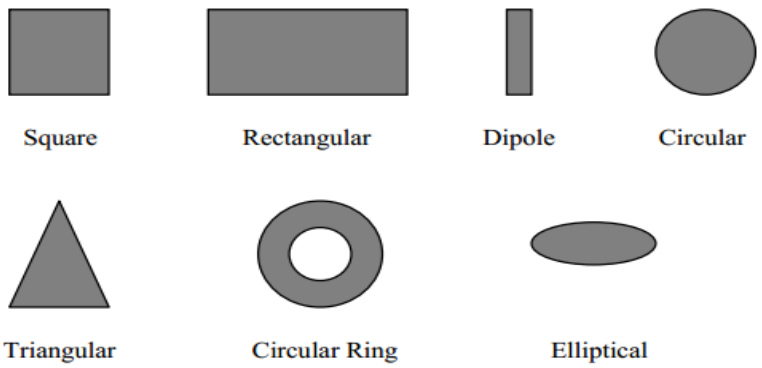

Figure 3.2: Different shapes of misrostrip patch element [7]

In a MPA, electric filed in the center of the patch is zero and the radiation is due to fringing field effect [7] between the patch and the ground plane. Fringing field is a function of the dimensions of the patch and the height of the substrate (*h*). Higher the substrate, the greater is the fringing field. The impedance bandwidth depends on the thickness (*t*) and dielectric permittivity $\mathcal{E}_r$ of the substrate. Thick substrate with low $\mathcal{E}_r$ increases the bandwidth. But if substrate thickness is increased, problem with antenna integration and surface-wave propagation can occur. Hence, bandwidth should be increased using other bandwidth enhancement techniques. There are numerous techniques available to enhance antenna's bandwidth which include multilayer structure antenna [34], microstrip antenna with an air-gap [35], microstrip antenna using parasitic elements [36, 37], log-periodic technique [38] , and also special shape and feeding techniques of microstrip antennas [39-41] [42].

3.2. Advantages and Disadvantages

Microstrip patch antennas have many advantages when compared to all non-planar antennas. Because of this, they are increasing in popularity and have usage in wide range of applications like mobile and compact devices, wireless communications, cellular phones, aircraft and satellite communications. Antennas for these types of applications need to be thin and

compact. Some of the principal advantages of patch antennas discussed by authors [7, 32] are given below:

- They are light and take up little volume.
- Low profile which makes them easy to adapt to different surfaces.
- Lower manufacturing costs and ease of making them in series.
- Supports both linear polarization and a circular polarization.
- Easily integrated to integrated microwave systems (MICs).
- They can be designed to work at different frequencies.
- They are mechanically robust to be mounted on hard surfaces [45, 46].

Despite several advantages, MPA suffers from various weaknesses as compared to other conventional antennas. Some of the important disadvantages discussed in [32, 47] are given below:

- Narrow bandwidth
- Low Gain
- Low efficiency
- Poor end fire radiator except tapered slot antennas
- Extraneous radiation from feeds and junctions
- Low power handling capacity.
- Surface wave excitation

3.3. Feeding Techniques

Several feeding technique are available for different types of MPA. They are divided into two categories: contacting and non-contacting [7]. In contacting feed method, as the name

suggests, the RF power is fed directly to the patch element by physical contact through a microstrip line. While in non-contacting, the power transfer between microstrip line and patch element is achieved through electromagnetic field coupling. Four widely used feed methods are microstrip line, coaxial probe (both contacting feed), aperture coupling and proximity coupling (both non-contacting feeds).

3.3.1 Microstrip Line Feed

In this feeding method, a conducting strip and the patch element are connected edge-to-edge, as shown in Fig. 3.3. Microstrip feed line is a conducting strip of much smaller width than the patch element. The advantage of this type of feed is that the strip can be etched on the substrate to make a planar structure.

The strip is easy to fabricate and simple to match by controlling its width and inset position. The purpose of the inset cut is to match the impedance of the microstrip line with that of the patch element without any other matching element. However, with the increase in substrate thickness, spurious radiation and surface waves also increase which limits the bandwidth of the patch antenna. The feed radiation also creates undesired cross polarization [7].

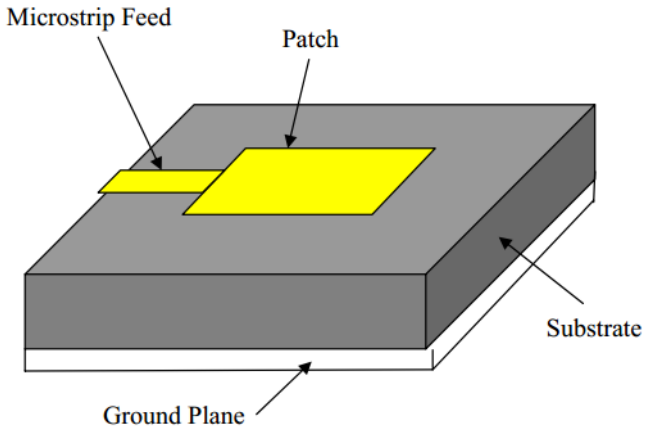

Figure 3. 3: Microstrip line feed [13]

3.3.2 Coaxial Feed

The coaxial feed, also known as probe feed, is a widely used feeding technique to feed MPAs. As shown in Fig. 3.4, the RF power is transferred through the inner conductor of a coaxial connector which is soldered to the back of the patch element through a hole in the substrate. The outer conductor is connected to the ground plane.

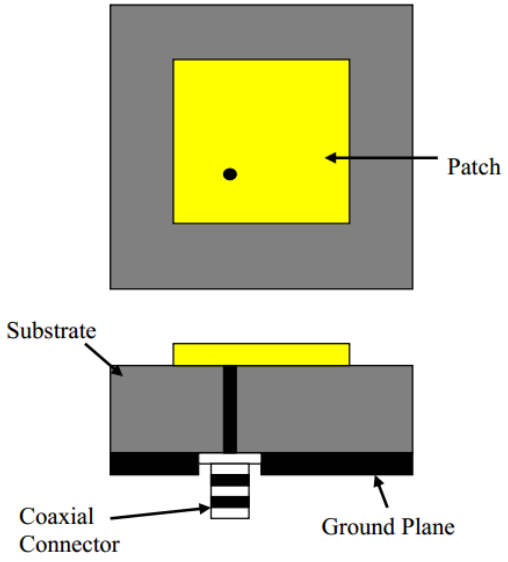

Figure 3. 4: Coaxial fed MPA [13]

The coaxial feed is easy to fabricate and has very low spurious radiation than microstrip line feed. The coaxial probe is easy to place over any desired point on the patch element in order to match the input impedance. However, the coaxial feed provides narrow bandwidth which is its major disadvantage. Also, it is difficult to model because it requires a hole to be drilled in the substrate. The connector sticks out outside the ground plane, as seen in Fig. 3.4, which does not make antenna completely planar. The probe length makes feed inductive which leads to the mismatching problem of impedance [32]. This problem is worse when thick substrates ($h>>0.02\lambda_0$) are used [6]. It is clear that despite ease of design and fabrication both of the

contacting feed methods suffer from various disadvantages. The two non-contacting feed methods, discussed below, solve many of these problems.

3.3.3 Aperture Coupled Feed

In aperture coupled feeding, there are two substrates separated by a ground plane. On the bottom side of lower substrate there is a microstrip feed line which couples energy to the patch element through a slot or an aperture in the ground plane that separates the two substrates. The feed arrangement is shown in Fig. 3.5.

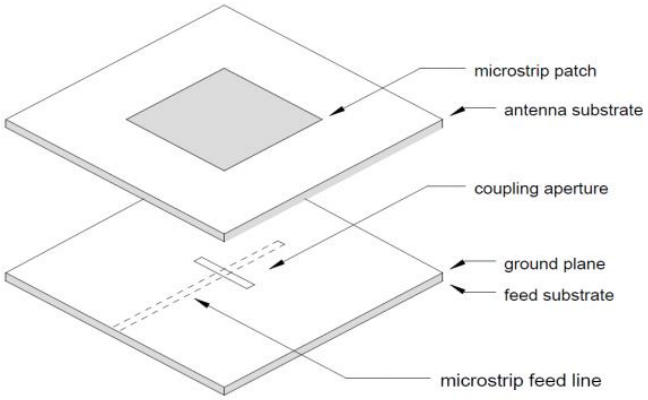

Figure 3. 5: Aperture coupled feed [13]

This feed method provides independent optimization of the feed mechanism and patch element. The coupling slot is centered under the patch, leading to cross polarization due to symmetry of the arrangement. The shape, size and location of the slot determine the amount of coupling from feed-line to the patch. The separation between the ground plane and the patch minimizes the spurious radiation. Usually, a thick and low $\mathcal{E}_r$ material is used for the upper substrate and a substrate with high $\mathcal{E}_r$ is used to optimize the radiation from the patch [7]. This feed configuration is difficult to fabricate, multiple layers increase antenna thickness and provides narrow bandwidth.

3.3.4 Proximity Coupled Feed

In proximity coupled feed, two dielectric substrates are used in an arrangement that feed line is sandwiched between two substrates and the patch element is on top of the upper substrate. The ground plane lays at the bottom of the lower substrate, as shown in Fig. 3.6. This type of feeding is also known as electromagnetic coupling scheme [6-7].

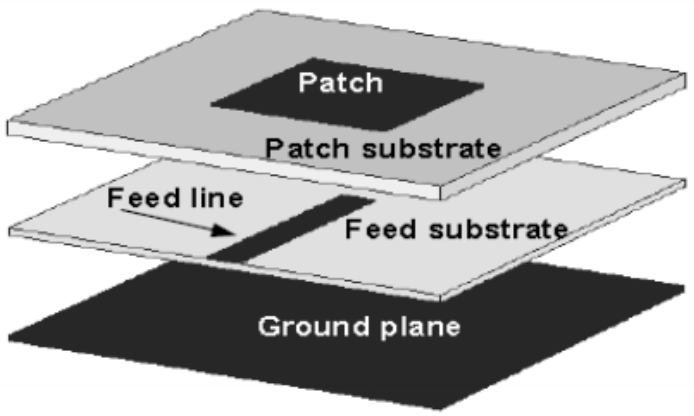

Figure 3.6: Proximity Coupled Feed [14]

Compared to the other three feed models, proximity coupled feed offers high bandwidth (up to 13%) and very low spurious radiation [6]. This feed offers individual substrate choice for patch element and feed line to optimize the individual performance. The impedance matching is done by controlling the length of the feed-line and width-to-line ratio of the patch. The major disadvantages are difficult fabrication due to complex structure and increase in overall thickness of the antenna.

3.4 Patch Antenna Design using Transmission Line Model

In this section, the design procedure for a rectangular MPA using transmission-line method [6-7] is discussed. The transmission-line model is a method for the analysis of the MPA

and the field distribution of all TM_{00n} modes. The model is not accurate but is simple and gives relatively good physical understanding of the nature of a microstrip patch antenna [6-7].

This model represents a rectangular patch as a parallel-plate transmission line connecting two radiating slots or apertures each of width *W* and height *h*, as shown in Fig. 3.7. In Fig. 3.7, *z* is the direction of propagation of transmission line. The microstrip is a non-homogeneous line of two dielectrics; substrate and air. The two slots represent high impedance termination (open-circuit) on both sides of the transmission-line. Therefore, depending on its length *L*, this structure has highly resonant characteristics.

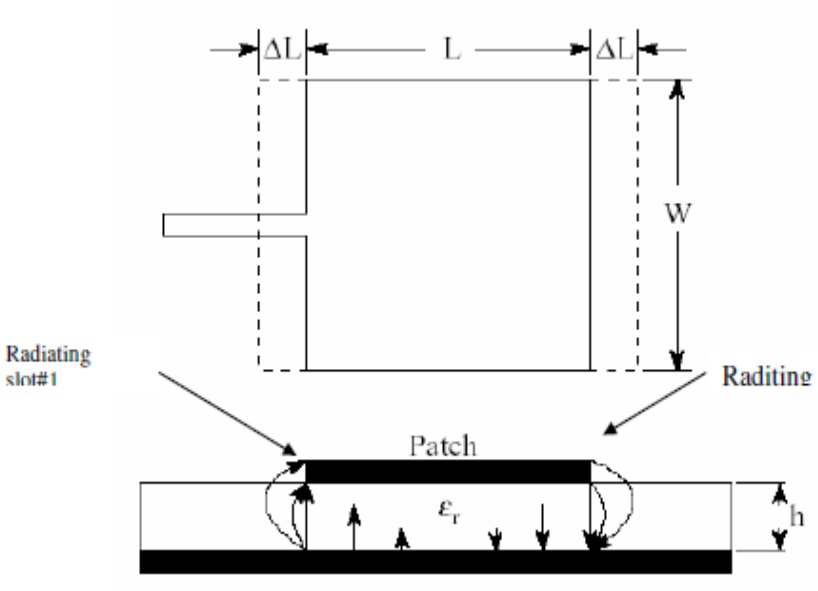

Figure 3. 7: Transmission-line model of the rectangular MPA [7]

In Fig. 3.7, it is shown that most of the field lines reside inside the substrate with some lines outside the patch in air. The transmission-line cannot support pure transverse electro-magnetic (TEM) mode of transmission because phase velocities are different in the substrate and air. So, the mode of propagation in this case would be quasi-TEM mode. The quasi-TEM mode occurs when the phase velocity of the EM wave is not constant because of two different

mediums (air and the substrate in this case). Hence, effective dielectric constant, ε_{reff}, must be considered in order to account for the fringing fields. The fringing fields are not completely confined inside the substrate but are also spread in air. Hence, the value ε_{reff} is slightly less than ε_r, and is given by Balanis [7] as:

$$\varepsilon_{reff} = \frac{\varepsilon_r+1}{2} + \frac{\varepsilon_r-1}{2}\left[1+12\frac{h}{w}\right]^{0.5} \quad (3.1)$$

Where ε_{reff} = effective dielectric constant

ε_r = dielectric constant of substrate

h= height of dielectric substrate

W= width of the patch

For the antenna to operate in the fundamental TM_{10} mode, the length of the patch element should be slightly less that $\lambda/2$, where λ is wavelength in dielectric medium and is given as $\lambda_0/\sqrt{\varepsilon_{reff}}$ and λ_0 is the wavelength in air. The TM_{10} mode implies that the field varies $\lambda/2$ cycle along the patch length and no variation occurs along patch width [6-7].

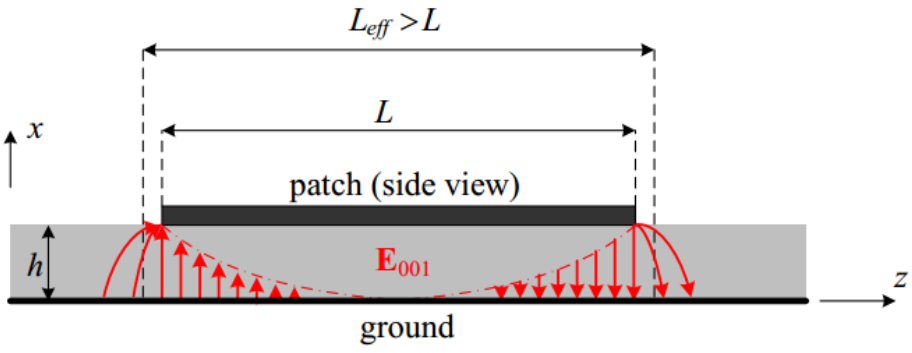

Figure 3. 8: Effect of fringing fields on the length of the patch element [13]

Figure 3.8 shows that because of the fringing fields, the resonant length of the patch is not equal to the physical length *L*. The dimensions of the patch on each end along its length have been increased by distance ΔL, thus $L_{eff} > L$. ΔL is given by Hammerstad [20]as:

$$\Delta L = 0.412h \frac{(\varepsilon_{reff}+0.3)\left(\frac{W}{h}+0.264\right)}{(\varepsilon_{reff}-0.258)\left(\frac{W}{h}+0.8\right)} \tag{3.2}$$

The effective length of the patch L_{eff} becomes:

$$L_{eff} = L + 2\Delta L \tag{3.3}$$

For a given resonance frequency f_0, the effective length L_{eff} is given as [17]:

$$L = \frac{c}{2f_0\sqrt{\varepsilon_{reff}}} \tag{3.4}$$

The resonant frequency f_0 of the rectangular MPA at any TM_{nm} mode is given by James and Hall [46] as:

$$f_0 = \frac{c}{2f_0\sqrt{\varepsilon_{reff}}}\left[\left(\frac{m}{L}\right)^2 + \left(\frac{n}{W}\right)^2\right]^{\frac{1}{2}} \tag{3.5}$$

where *m* and *n* are modes along *L* and *W* respectively.

The patch width *W* is given by Bahl and Bhartia [47] as:

$$W = \frac{c}{2f_0\sqrt{\frac{(\varepsilon_r+1)}{2}}} \tag{3.6}$$

Theoretically, the patch antenna designing using transmission line method requires an infinite ground plane. But for practical applications, it is impossible to achieve an infinite ground plane. However, it has been proved by the research [32] that similar results can be achieved with a finite ground plane if its size is greater than the patch size by six times the substrate thickness in all dimensions [6]. Hence, the formulas for the ground plane dimensions can be written as:

$$L_g = 6h + L \tag{3.7}$$

$$W_g = 6h + W \tag{3.7}$$

Where L_g=length of groud plane

W_g = width of ground plane

CHAPTER 4: ANTENNA DESIGN AND SIMULATION RESULTS

In this chapter, design procedure of a microstrip patch antenna (MPA) for 802.11ac Wi-Fi application is discussed in detail which initiates with designing a microstrip rectangular patch antenna that can operate at 5GHz WLAN band and facilitates the features that conform to the 802.11ac Wi-Fi standard [1]. The MPAs have gained tremendous importance because of their low-profile, compact size and fabrication ease [7, 38, 48]. The simulation of the proposed antenna is performed on two different software platforms i.e. Agilent Advanced Design System (ADS) [49] and CST microwave studio [50]. ADS system is an electromagnetic simulator. Its tool of simulation depends on full-wave "Method of Moment" (MoM) numerical technique [30-31]. This study also presents the comparative analysis of the simulation results on two different software platforms based of different techniques i.e. MoM and FDTD. The antenna is designed on two different substrates, a high end i.e. Rogers 6010.2LM [51] and a low end i.e. FR4 [59] substrate to analyze performances between both.

4.1 Initially Designed Single Element Patch Antenna

Selection of substrate is the initial and most crucial step towards the designing of patch antenna. For this project, Rogers 6010.2LM [51] laminate was initially selected in the designing of the patch antenna. The dielectric constant and height values chosen for the substrate are ε_r = 10.2 and h = 1.9mm, respectively. To meet the requirement of performance and bandwidth, these values are selected carefully, as the antenna's performance depends highly on the selection of dielectric material. Thin substrates are required to achieve compactness, but as a result of height reduction, the patch antenna's bandwidth decreases [46]. Furthermore, patch size can be reduced by increasing the value of ε_r but antenna's bandwidth reduction will follow too [47].

So, a careful transaction and ratio maintenance must be done between antenna's size and its performance. The f_r for the rectangular patch was selected to be 5.0 GHz. The initial calculations of the patch antenna were performed using transmission line model [7] and Line Calc tool in ADS [49] is used to compute the characteristic impedance of the line. The empirical formulas presented in chapter 3 (section 3.4) are used here to obtain the initial parameters of rectangular MPA for 802.11ac Wi-Fi application. The inputs to these formulas are the values of ε_r, h and the desired frequency (f). All the respective formulas and calculated results are given below in Eq. (1) – (5):

$$L = L_{eff} - 2\Delta L = 8.8305\text{mm} \tag{1}$$

Where,

$$L_{eff} = \frac{c}{2f\sqrt{\epsilon_{reff}}} = 10.38\text{mm} \tag{2}$$

$$\epsilon_{reff} = \frac{\epsilon_r+1}{2} + \frac{\epsilon_r-1}{2}\left[\frac{1}{\sqrt{1+12\frac{h}{W}}}\right] = 8.349 \tag{3}$$

$$\Delta L = 0.412h\frac{[\epsilon_{reff}+0.3]\left[\frac{W}{h}+0.264\right]}{[\epsilon_{reff}-0.258]\left[\frac{W}{h}+0.8\right]} = 0.776\text{mm} \tag{4}$$

$$W = \frac{c}{2f}\sqrt{\frac{2}{\epsilon_r+1}} = 12.67\text{mm} \tag{5}$$

The geometry of the basic patch antenna is shown in Fig. 4.1 below. For initial simulation of the MPA the incorporated feeding technique was Inset feed [52]. To analyze the antenna, the Agilent ADS helps us to get information about various parameters of the antenna such as

reflection coefficient, VSWR, directivity, gain, 2D and 3D radiation patterns, impedance loop plot on smith chart and current distribution. The designed antenna was simulated on ADS Momentum which results in the bandwidth of around 90MHz and return loss of around -14 dB which is shown in Fig. 4.2. But as proposed antenna is specific to the application, so it would best cater if achieved bandwidth is around 100-160MHz, so few changes were made in order to cater for the issues that were observed after initial simulation.

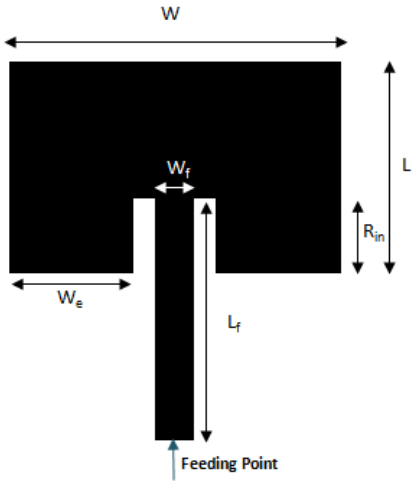

Figure 4. 1: Layout of the initially designed patch antenna

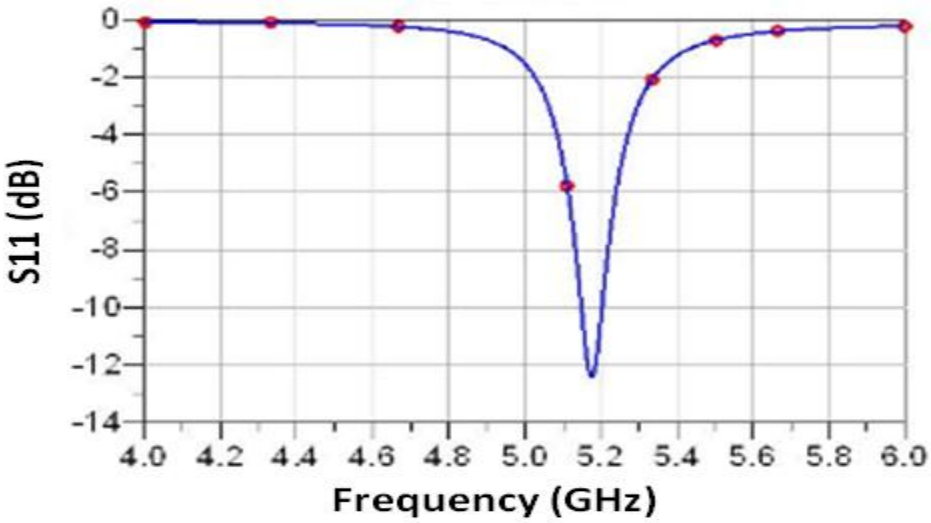

Figure 4. 2: Initially designed patch antenna reflection coefficient – S_{11}

As claimed by the authors in [53], the design formulas give approximate antenna design parameters. These parameters can serve as a good starting point to achieve the desired antenna performance. In the following section, the optimized antenna is presented along with its results.

4.2 Proposed Structure of Single Element Patch Antenna

In this section, the simulation results of an optimized single element rectangular MPA are presented. Each of the steps were done one-by-one and its effect was observed on the antenna performance by making repeated simulations. The geometry of the modified structure is shown in Fig. 4.3 and all the dimensions are summarized in Table 6. Where in Table 6, R_{in} is the resonant input impedance of the antenna, L_f and W_f are the single element microstrip antenna feed-line length and width respectively and L_s and W_s are the length and width of the two symmetrical slits in the patch as shown in Fig. 4.3. The length (L) and width (W) of patch were optimized to get the best possible results.

In order to widen the band so as to get the desired bandwidth the edges of the main patch were tapered [41] and two symmetrical slits were added to the rectangular patch [65]. All the results are discussed in detail in next section. In this proposed design, modified form of inset feed is used to make the performance of antenna even better [54]. In this design we used a modified inset fed patch antenna as an effort to help antenna performances towards further improvement. This research presents the proposition of modified inset fed patch antenna based on the concept of both (inset fed patch antenna) and (gap coupling) [54-55].

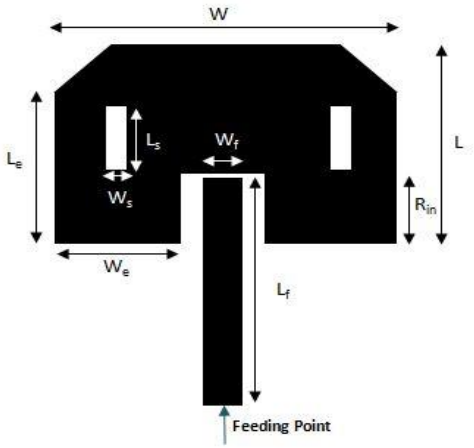

Figure 4. 3: Layout of the proposed antenna design for 802.11ac Wi-Fi application

Table 6: Dimensions of optimized single element rectangular patch antenna (Unit: mm)

Rectangular Microstrip Patch Antenna								
W	L	L_f	W_f	L_s	W_s	L_e	W_e	R_{in}
12.67	8.6	9.55	1.97	3.03	0.78	6.7	4.55	3.17

4.3 Feeding Technique

Now, we present a modified inset-fed patch antenna as an effort to help antenna performances towards further improvement. The inset-fed MPA is to move the feed point to a lower impedance region inside the patch [46]. The feeding method of the modified gap coupling [55] is narrow gap i.e. 0.2mm in this design; around the feed-line to the patch as shown in figure 4.3. The modified inset-fed patch antenna adopted capacitive coupling feed method based on the concept of inset-fed patch antenna so as to achieve reduce cross polarization level. The inset-fed patch antenna feeds the patch from its radiating edge with an appropriate amount of inset for easily realized impedance matching. The purpose of the modified inset-fed antenna is to achieve

perfect impedance matching corresponding among the microstrip line and the patch antenna. In Figure 4.3, the modified inset-fed patch antenna's geometry is shown. Distributed field between the patch and the ground plane determines the radiation from microstrip antenna. Current distribution on the patch is also an explanation of this. The current distribution of the designed MPA on ADS is demonstrated in Fig. 4.4.

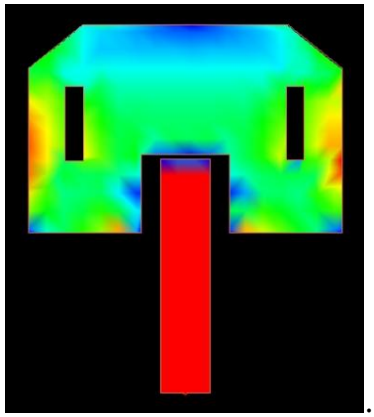

Figure 4. 4: Surface current distribution of the designed MPA

4.4 Simulation Results of Single Element on ADS Momentum

The antenna parameter which is of significant importance in the antenna design is the return-loss which defines the bandwidth and the impedance matching characteristic. The initial simulation of the MPA on ADS resulted in a bandwidth of around 90MHz and return-loss of -14dB. Few changes were made to the design, so as to make an efficient device. After making precise changes to the dimensions and tapering the edges of the main rectangular patch, the band was widened and the achieved bandwidth was 170MHz which was desired for the 802.11ac Wi-Fi application. The simulated return-loss curve of the designed MPA on ADS momentum is shown in Fig. 4.5.

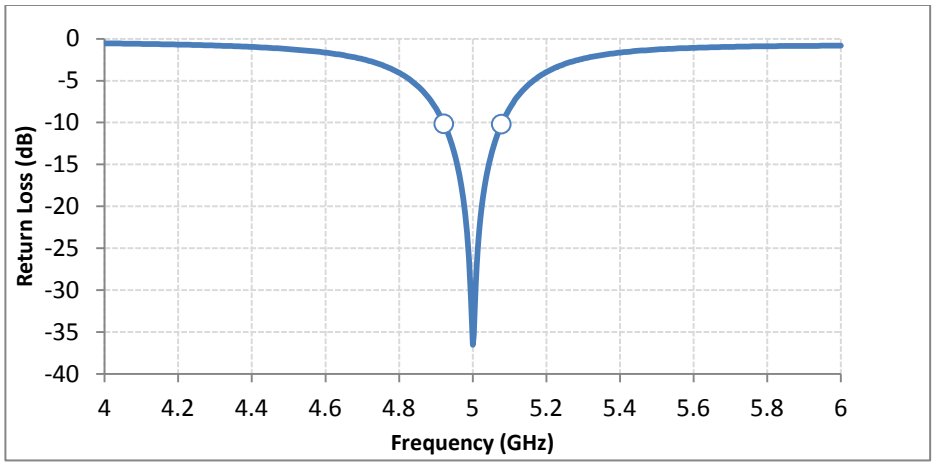

Figure 4. 5: S_{11} of the single element antenna on ADS momentum

It can be seen from Fig. 4.5 that the resulted return-loss of the designed antenna on ADS momentum at the desired f_r of 5GHz is below -10dB which is a good approximation for the design. This is directed to the fact that the reflected signal is less than 10% of what was transmitted. By incorporating modified inset feed, the proposed antenna can attain improved return loss i.e. around -37dB than original inset fed antenna at f_r =5.0GHz.

Fig. 4.6 shows the antenna gain and directivity. Gain at 5GHz is 6.5dBi. The antenna has an efficiency of 85% at 5GHz, as shown in Fig. 4.7.

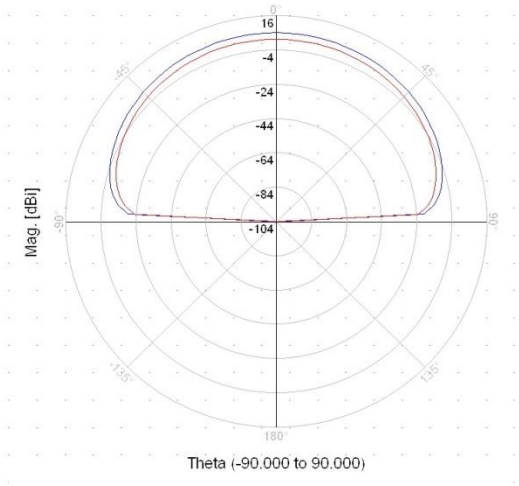

Figure 4. 6: Rectangular patch single element antenna gain and directivity at 5GHz

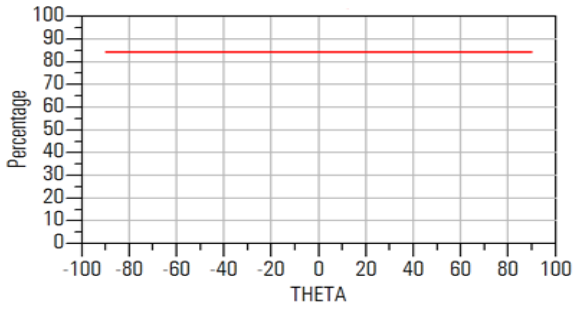

Figure 4. 7: Rectangular single element patch antenna efficiency at 5GHz

4.5 2x4 Rectangular Patch Array

After designing the single element antenna that is performing well over the frequency range of 802.11ac, the 8-element MIMO antenna array is designed and its configuration is shown in Fig. 4.8, where the dimensions of each of its elements are exactly as same as in Fig. 4.3 with reference to Table 6 and named from element-1 (*E1*) to element-8 (*E8*) respectively. These elements are fed individually by their perforated ports where these elements are separated edge-to-edge by 5mm [56]. The theoretical and analytical studies about the effect of inter-element distance on the capacity of MIMO systems are discussed in [57-58] which show that for MIMO antennas, maximum efficiency can be attained at an inter-element distance of 0.4λ or above. However, good results have been obtained at a separation of 5mm [56].

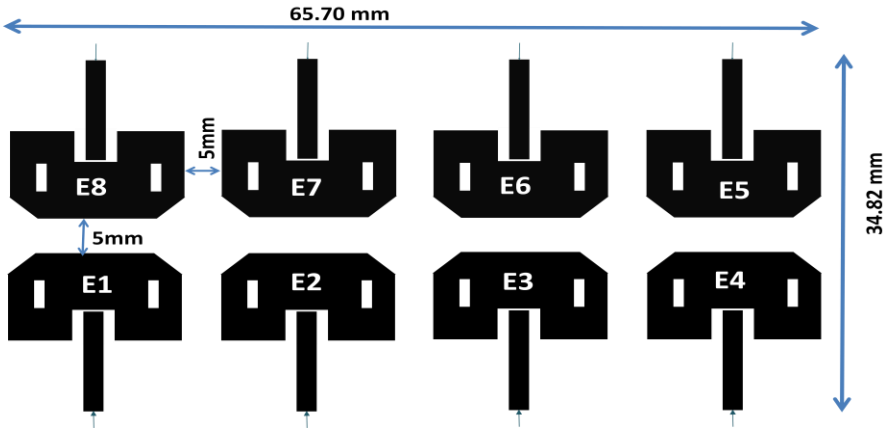

Figure 4. 8: 8-element rectangular patch antenna array using RT/Duroid 6010.2LM substrate

The reflection coefficient plots for each of the element in the the 2 x 4 array antenna are shown in Fig. 4.9. The values of the reflection coefficient of eight elements S_{11}-S_{88} at 5GHz frequency are -21dB, -37dB, -21dB, -53dB, -37dB, -21dB, -21dB and -53dB, respectively. These values reflect very good impedance matching for the 2x4 array antenna configuration. It can be seen from Fig. 4.9(a) and Fig. 4.9(b) that the antenna elements resonates between 4.985–5.15GHz with a -10dB bandwidth of 140MHz.

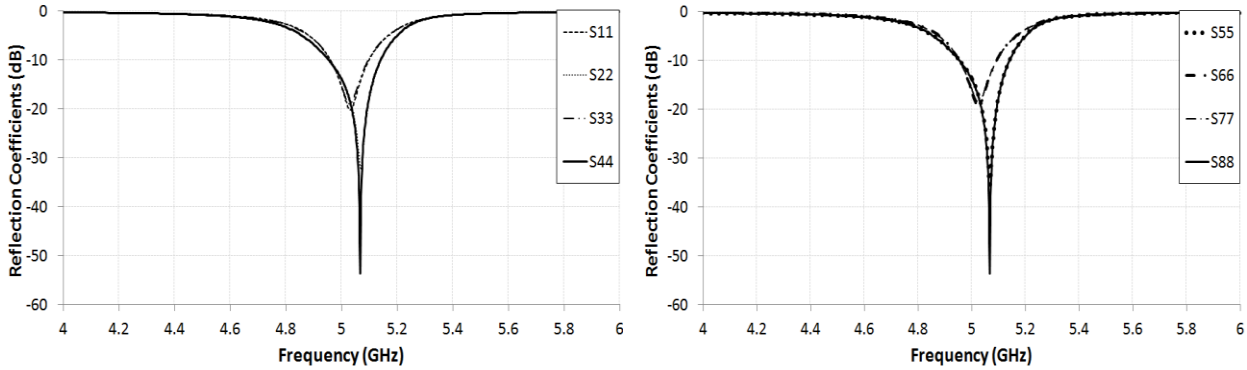

(a) (b)

Figure 4. 9: Reflection coefficients $-S_{11}$-S_{88} of 2 × 4 rectangular patch antenna array using RT/Duroid 6010.2LM substrate (a) S_{11}-S_{44} (b) S_{55}-S_{88}

While designing a MIMO antenna system, another important performance evaluation parameter is the isolation between the antenna elements. The isolation curve between the antenna elements of the designed MIMO antenna system using MoM technique is simulated and results are summarized in Fig. 4.10. In Fig. 4.10, only the isolation between *E1* with rest of the antenna elements is shown. It can be observed from Fig. 4.10 that good isolation characteristic and an isolation of around 8dB is achieved from the proposed 8-element MIMO antenna system.

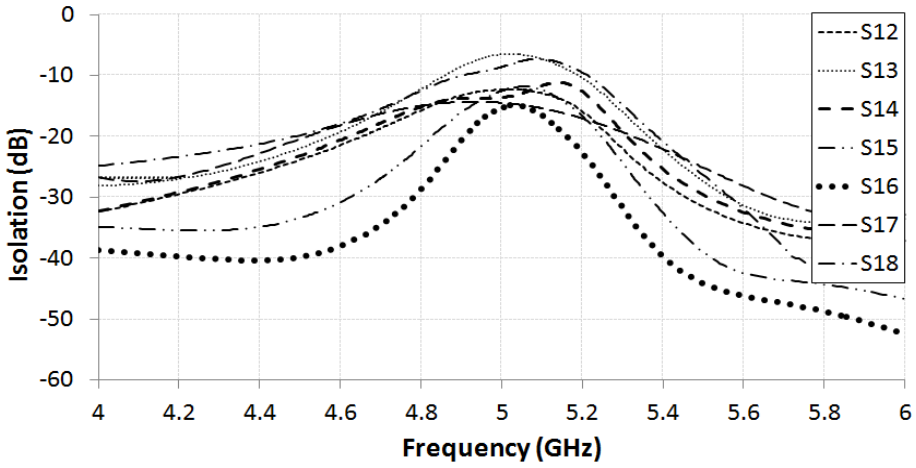

Figure 4. 10: Isolation between *E1* with adjacent antenna elements *S12 -S18* using ADS (MoM technique)

The antenna has an efficiency of 97%, as shown in Fig. 4.11, which suggests an excellent radiated to input radio-frequency power ration.

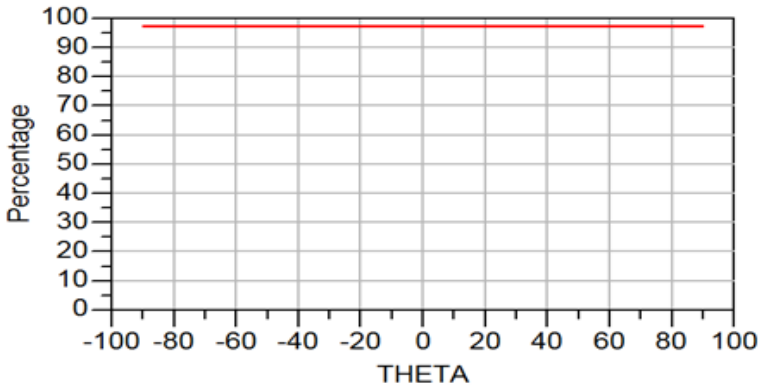

Figure 4. 11: Efficiency of 2x 4 rectangular patch antenna array using RT/Duroid 6010.2LM substrate at 5GHz

The 2D radiation patterns of the designed 8-element MIMO antenna array at 5GHz are shown in Fig. 4.12 (a-b) using FDTD technique. It can be observed from Fig 4.12 (a-b) that main lobe magnitude of around 6.7dBi and side-lobe level of around -11dB is achieved for all the antenna elements of the array at the 5GHz band of operation.

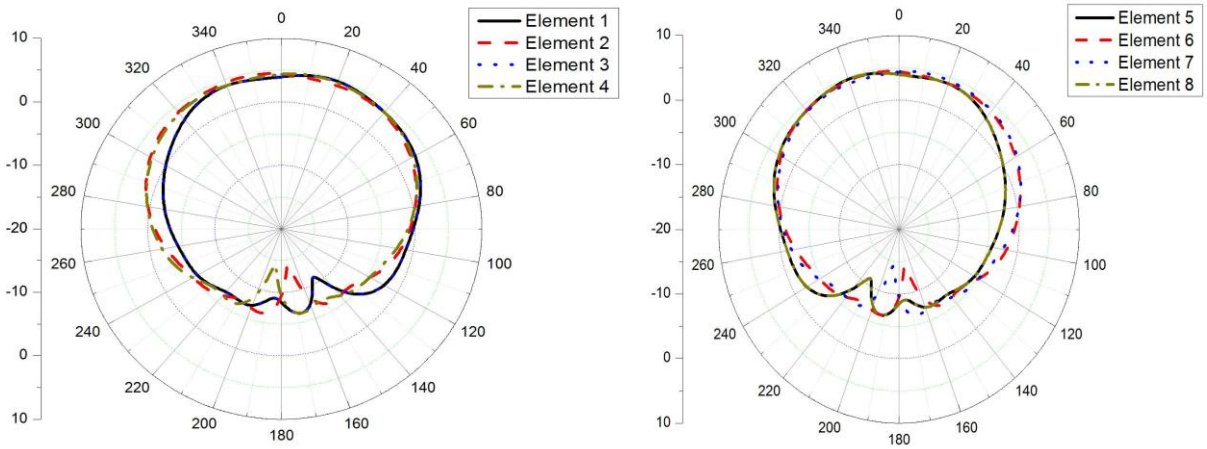

(a) (b)

Figure 4. 12: Simulated 2D radiation pattern of the 8-element MIMO array using CST (FDTD technique) (a) E1 to E4 and (b) E5 to E8 radiation patterns

3D-Radiation patterns of designed MIMO antenna system at 5GHz is show in Fig. 4.13 on ADS which reflect that at the desired frequency i.e. 5GHz, radiation pattern is stable.

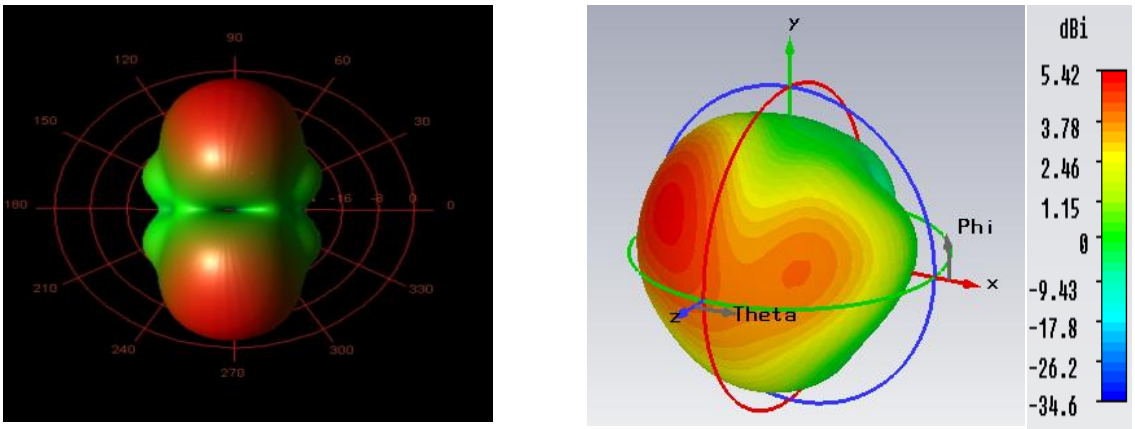

(a) (b)

Figure 4. 13: Simulated 3D radiation pattern of the 8-element MIMO array using (a) ADS (b) CST Microwave studio

CHAPTER 5: COMPARATIVE ANALYSIS

This chapter presents the comparative study of the measured and simulated results of the designed 8-element MIMO antenna system as well as difference in performance of a high and a low-end substrate i.e. Rogers 6010.2LM [51] and FR-4 [59]. Also, comparative analysis of the simulation results using two different techniques i.e. MoM and FDTD methods are also discussed in this chapter.

5.1 Comparative analysis of the MoM and FDTD techniques

The proposed MPA element shown previously in Fig. 4.3 (Chapter-4) with dimensions given in Table 6 was designed on CST microwave studio [50] as well in order to evaluate the performance of two very well known techniques available for electromagnetic computation i.e. MoM and FDTD. The simulated S_{11} curves of the designed single antenna element using MoM [49] and FDTD [50] modeling techniques are shown in Fig. 5.1 below.

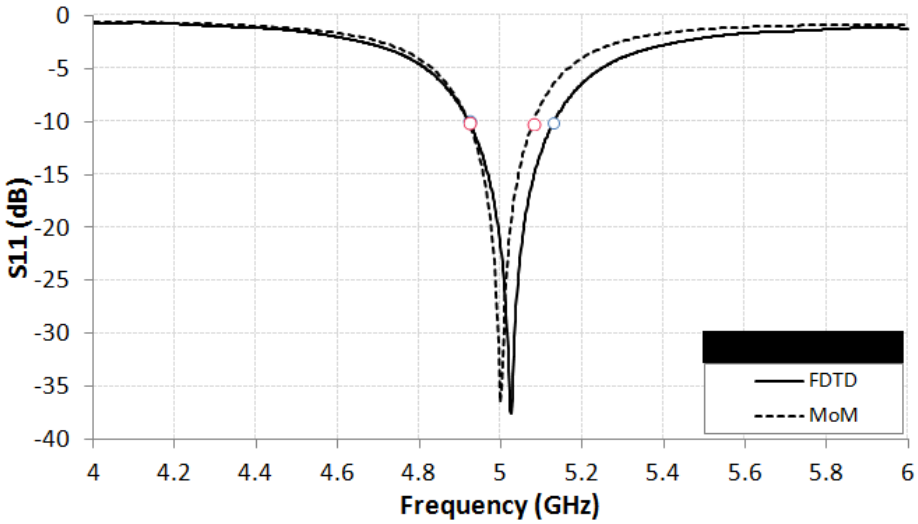

Figure 5. 1: Comparison of the S_{11} curves of the designed single antenna element using ADS momentum (MoM technique) and CST microwave studio (FDTD technique)

The results in Fig. 5.1 suggest that the two techniques resulted in quiet similar outputs except that of the bandwidth. It can be observed from Fig. 5.1 that better performance in terms of bandwidth is achieved with FDTD method as compare to the MoM technique. The achieved bandwidth with FDTD technique is 205MHz whereas with MoM its around 170MHz. As far as the antenna gain and directivity is concerned, the gain and the directivity of the designed single MPA element, when simulated on ADS is shown in Fig. 5.2(a) below.

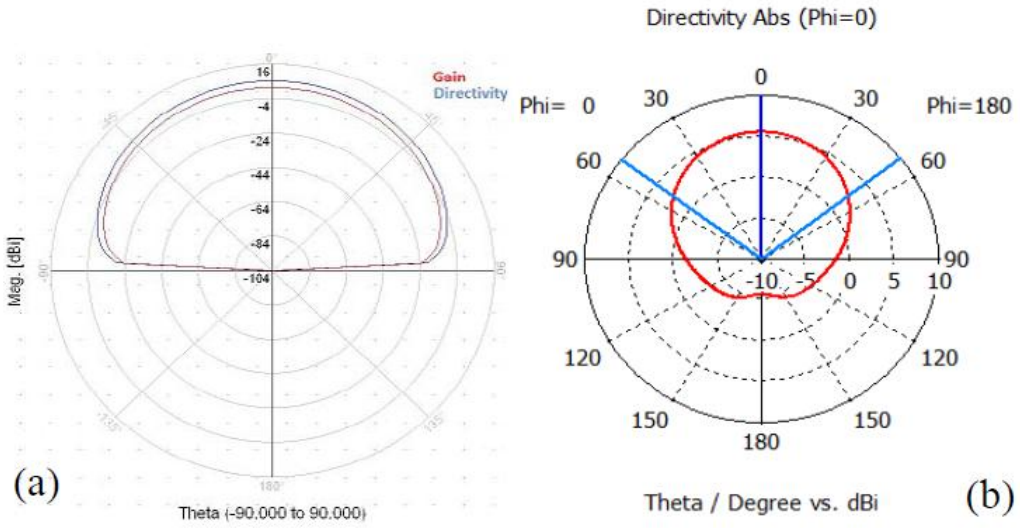

Figure 5. 2: Gain of the designed single antenna element at 5GHz band (a) Using ADS (MoM technique) and (b) Using CST (FDTD Technique)

It can be seen from Fig. 5.2(a) that the achieved gain is 6.5dBi at 5GHz band when simulated on ADS and it doesn't show any back lobe radiation which is due to the fact that ADS assumes infinite ground plane. Whereas in case of CST, there is a requirement to define a finite ground plane which leads to the back lobe radiations as highlighted in Fig. 5.2(b). The achieved gain using CST was 5.4dBi for the same antenna as can be observed in Fig. 5.2(b). A similar 8-element MIMO system was designed using CST as shown previously in Fig. 4.8 (Chapter-4). The simulated reflection coefficients S_{11}- S_{88} curves of the designed MPA using MoM and FDTD

modeling techniques are shown in Fig. 5.3(a-d). In the single-element antenna simulations, both techniques i.e. MoM and FDTD showed quite similar results, but in case of MIMO antenna simulation, results achieved by MoM were better than the ones obtained by the FDTD technique.

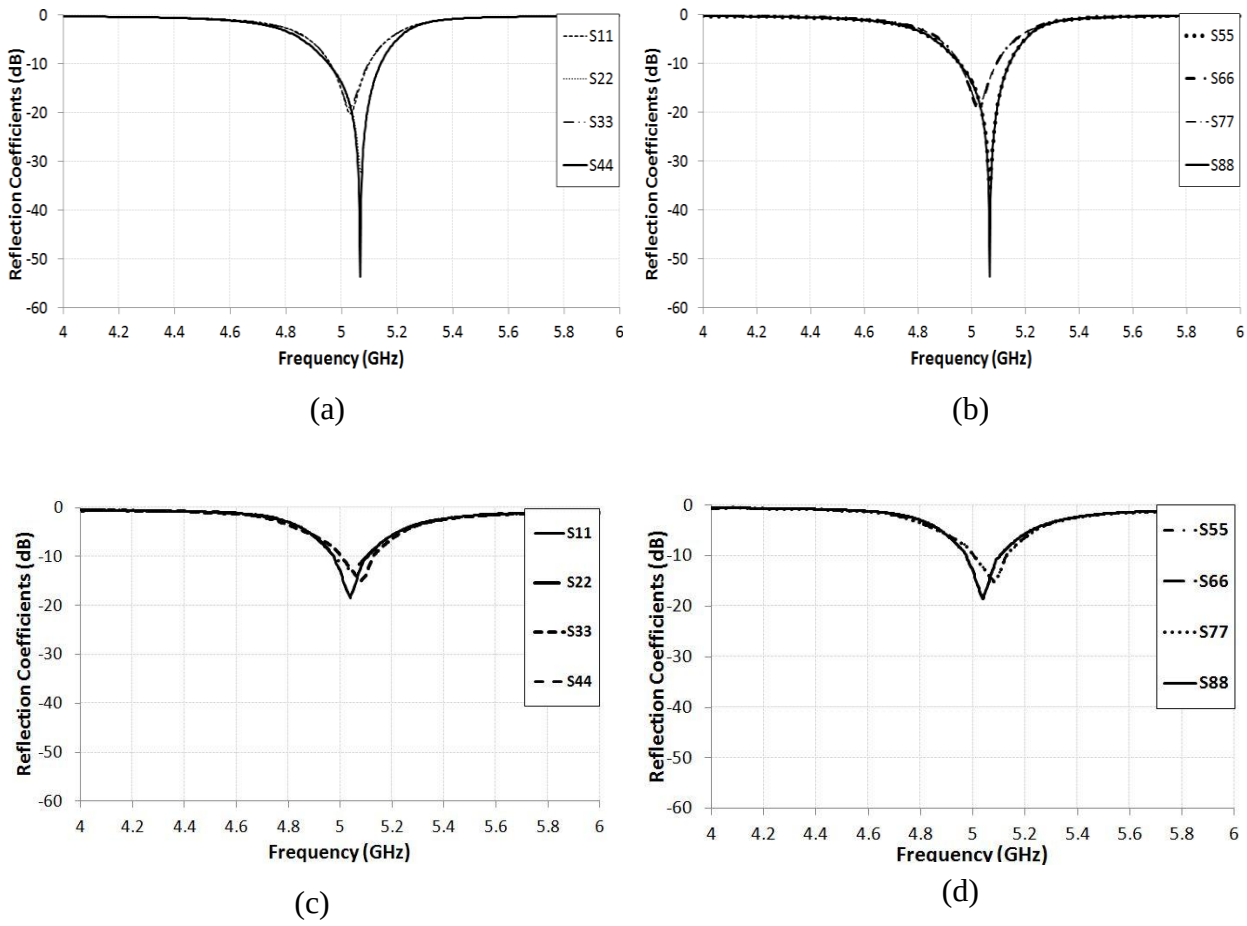

Figure 5. 3: Comparison of the reflection coefficients of the 8-element MIMO antenna array using (a) S_{11}-S_{44} −ADS momentum (MoM technique) (b) S_{55}-S_{88} −ADS momentum (MoM technique) (c) S_{11}-S_{44}−CST microwave studio (FDTD technique) (d) S_{55}-S_{88} −CST microwave studio (FDTD technique)

The proposed MIMO antenna array design was simulated and verified using both ADS based on MoM and CST based on FDTD techniques. Both the techniques verified the design and

it was observed that when multiple i.e. 8 designed MPA elements were assembled in the form of an array, there was an increase in antenna directivity i.e. 10.8dBi and 6.7dBi was achieved for MoM and FDTD techniques respectively. Attained bandwidth of proposed 8-element MIMO antenna system using MoM is 140MHz whereas FDTD technique resulted an operating band of 131MHz. Moreover, better reflection coefficients were obtained using MoM as compare to FDTD method. Comparative analysis of results using FDTD technique and MoM technique is shown in Table 7.

Table 7: Comparative analysis of the 8-element MIMO antenna array using the MoM and FDTD techniques (Substrate Used: RT/duroid 6010.2LM)

2 x 4 MIMO Antenna Array for 802.11ac Wi-Fi applications									
		E_1	E_2	E_3	E_4	E_5	E_6	E_7	E_8
Centre Frequency (GHz)	**MoM**	5.07	5.02	5.02	5.07	5.07	5.02	5.02	5.07
	FDTD	5.02	5.04	5.04	5.09	5.04	5.02	5.04	5.02
Reflection Coefficient (dB)	**MoM**	-37	-21	-21	-53	-37	-21	-21	-53
	FDTD	-19	-14	-14	-15	-15	-19	-15	-19

5.2 Performance Evaluation of FR4 and Rogers 6010.2LM

In order to evaluate the performance of a high and a low-end substrate i.e. Rogers 6010.2LM [51] and Flame Resistant 4 (FR4) [59], the 8-element MIMO antenna array for 802.11ac Wi-Fi application was also designed on FR4 substrate. Initially, a single patch was designed on ADS momentum and was tuned to get the antenna parameters that conform to

802.11ac Wi-Fi application. The dimensions of the designed patch computed using transmission-line model are shown in Table 8, whereas the structure of the designed antenna along with surface current distribution is depicted in Fig. 5.4 (a) and 5.4(b) respectively. The transmission-line feed is used in this design to excite the MPA element.

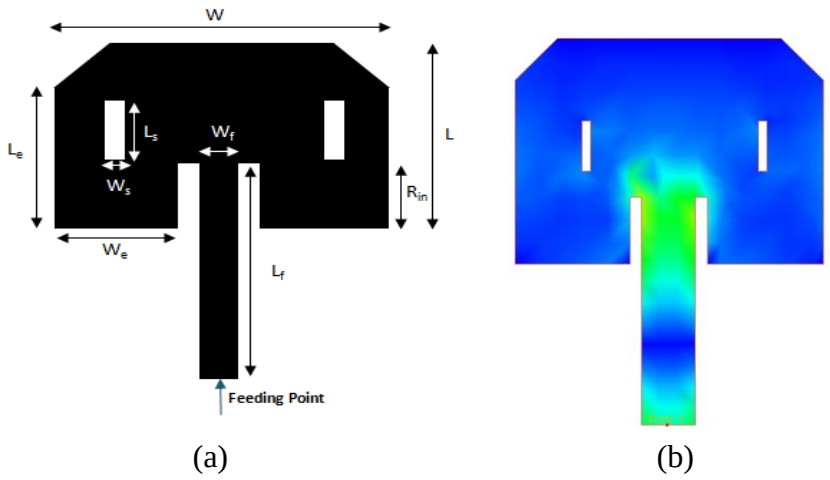

Figure 5. 4 : (a) Layout of proposed antenna design for 802.11ac Wi-Fi application (b) Surface current distribution for designed MPA

Table 8: Dimensions of single element rectangular patch antenna (FR4)

Rectangular Microstrip Patch Antenna								
W	***L***	***L_f***	***W_f***	***L_s***	***W_s***	***L_e***	***W_e***	***R_{in}***
17.94	13.40	13.55	3.12	3	0.5	10.89	6.79	4.0

The resulted S_{11} of designed single element MPA on FR4 is shown in Fig. 5.5. It can be seen from Fig. 5.5 that the S_{11} of the antenna on ADS momentum at the desired *fr* of 5GHz is below -10dB which is a good approximation for the design. Moreover it is observed that both substrates resulted in almost similar S_{11} i.e. -37dB and bandwidth of around 160MHz whereas

antenna designed using FR4 was larger in dimensions as compare to the one designed on Rogers 6010.2LM.

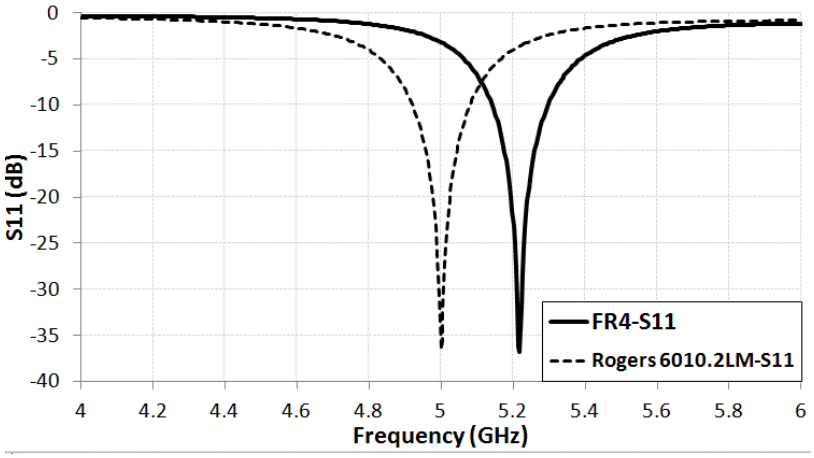

Figure 5. 5: Comparison of the S_{11} of designed MPA on FR4 and Rogers 6010.2LM substrates

The 2D and 3D radiation patterns of designed MPA on FR4 are shown in Fig. 5.6. It can be seen from Fig. 5.6 that the achieved gain is 5.7dBi at 5GHz band whereas with Rogers 6010.2LM substrate it was 6.5dBi.

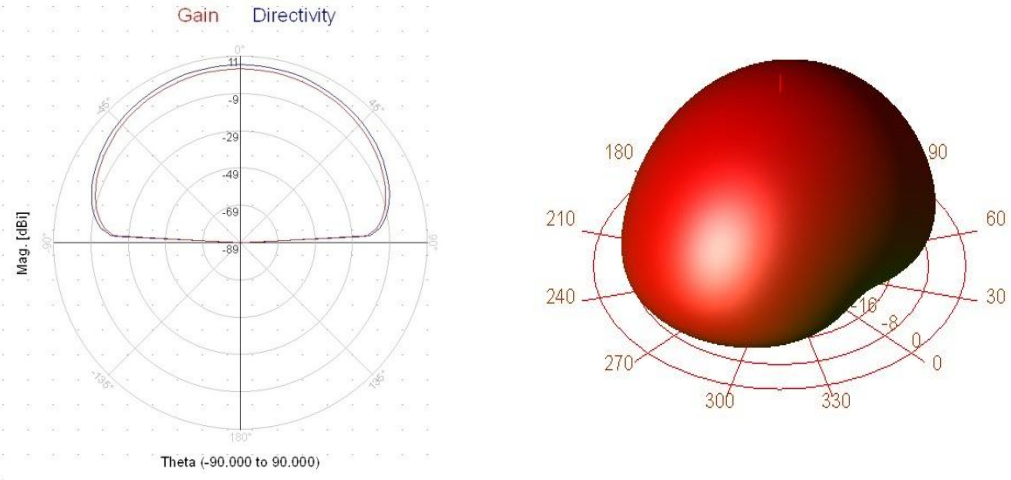

(a) (b)

Figure 5. 6: Radiation Patterns of the designed MPA on FR4 (a) 2D (b) 3D

An 8-element MIMO antenna array was designed to meet the 802.11ac requirements using the FR4 substrate. The designed antenna system is shown in Fig. 5.7 below.

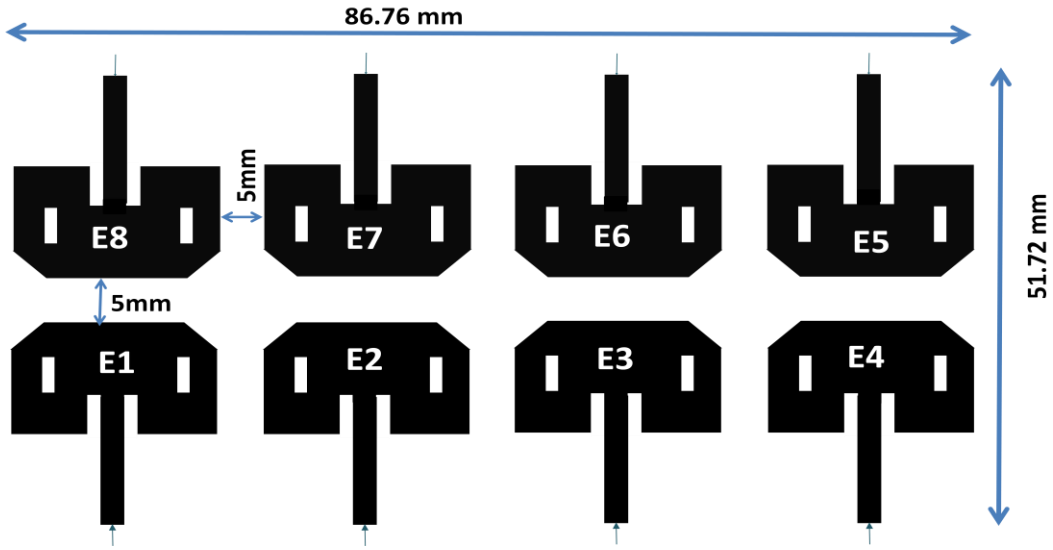

Figure 5. 7 : The 8-element rectangular patch antenna array using FR4 substrate

The reflection coefficient curves of all the array elements i.e. *E1-E8* are shown in Fig. 5.8(a-d) for FR4 and Rogers 6010.2LM substrates. It can be observed from Fig. 5.8 (a-d) below that better reflection coefficients were achieved when high dielectric substrate i.e. RT/Duroid 6010.2LM was used whereas low-end substrate i.e. FR4 resulted in better bandwidth than the one achieved with high-dielectric [51] substrate i.e. 140MHz, which is due to the fact that substrates having low $\mathcal{E}_r$ and more thickness cause an increase in the bandwidth. Antenna elements resonated between 5.131-5.308GHz with a -10dB bandwidth of 177MHz when FR4 was used. Comparative analysis of results using RT/duroid 6010.2LM and FR4 substrate is shown in Table 9.

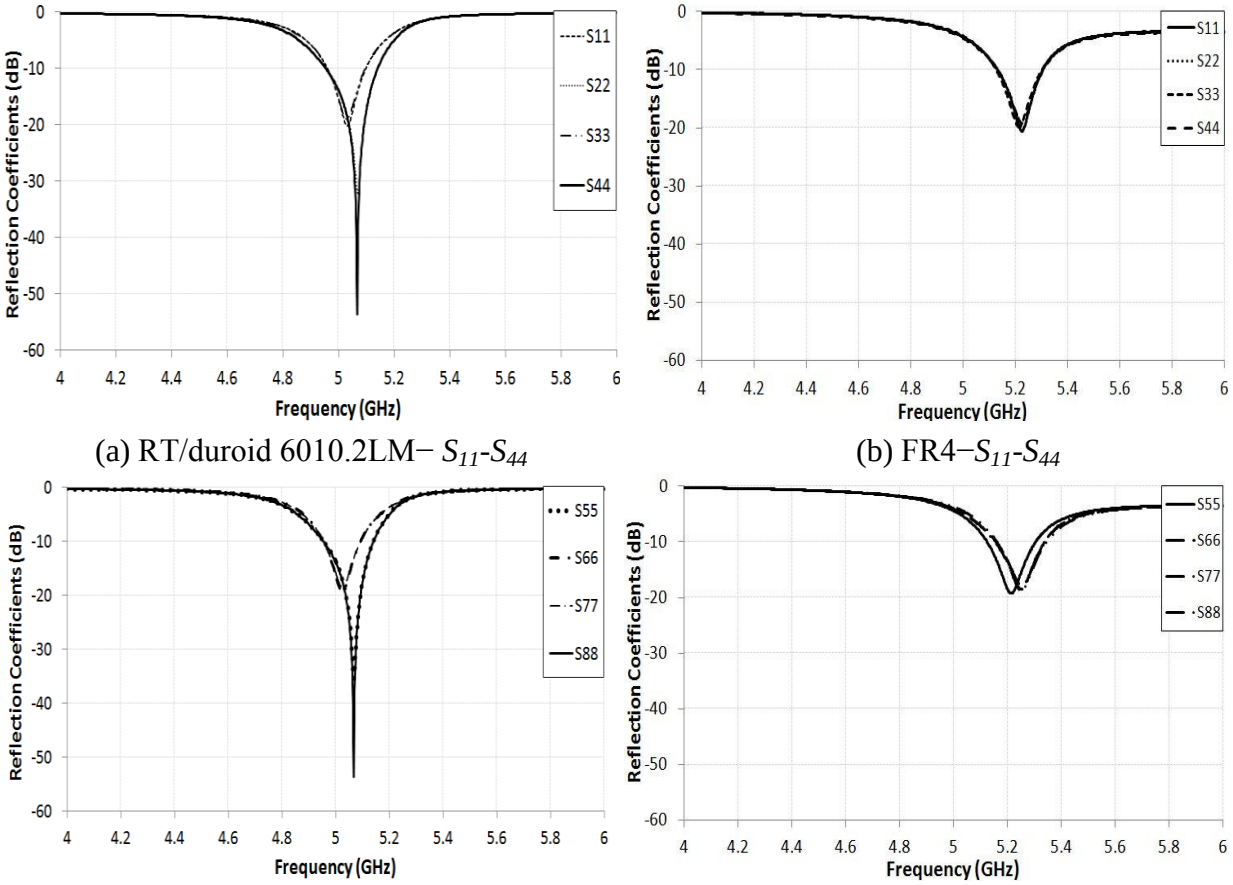

(a) RT/duroid 6010.2LM− S_{11}-S_{44}

(b) FR4−S_{11}-S_{44}

(c) RT/duroid 6010.2LM− S_{55}-S_{88}

(d) FR4− S_{55}-S_{88}

Figure 5. 8 : The 2 × 4 rectangular patch antenna array reflection coefficients (a) RT/duroid 6010.2LM– S_{11}-S_{44} (b) FR4− S_{11}-S_{44} (c) RT/duroid 6010.2LM− S_{55}-S_{88} (d) FR4− S_{55}-S_{88}

The 2D and 3D radiation patterns for the 8-element MIMO antenna system using FR4 substrate are shown in Fig. 5.9 (a) and (b) respectively. It can be observed from Fig. 5.9 (a) that achieved gain with FR4 substrate using MoM is 8.84dBi whereas the gain figure observed when antenna was designed on high dielectric substrate i.e. RT/Duroid 6010.2LM was 10.8dBi. Fig. 5.9 (b) depicts that 8-Element MIMO antenna system designed on FR4 substrate has good radiation characteristics.

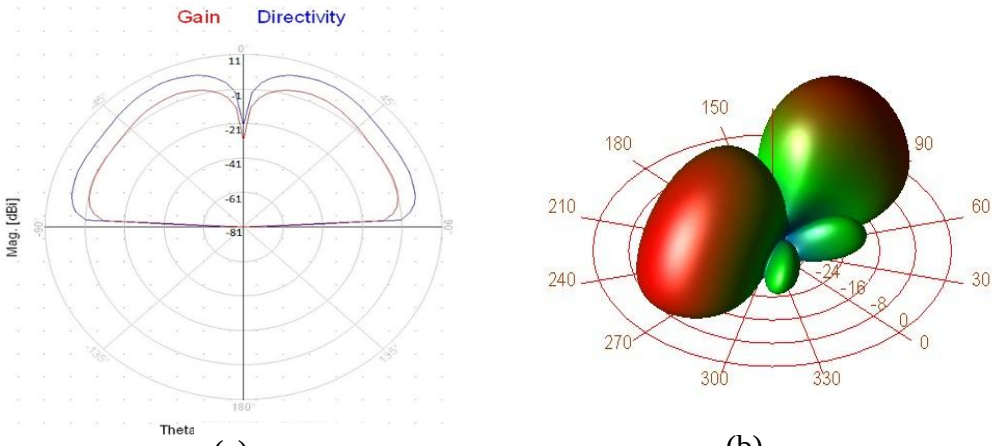

(a) (b)

Figure 5. 9: Radiation patterns of the designed 8-element MIMO antenna array on FR4 Substrate (a) 2D (b) 3D

Table 9: Comparative analysis of the 8-element MIMO antenna array using RT/duroid6010.2LM and FR4 substrates

2 x 4 MIMO Antenna Array for 802.11ac Wi-Fi applications									
		E_1	E_2	E_3	E_4	E_5	E_6	E_7	E_8
Centre Frequency (GHz)	**RT/duroid 6010.2LM**	5.07	5.02	5.02	5.07	5.07	5.02	5.02	5.07
	FR4	5.22	5.21	5.22	5.21	5.21	5.22	5.21	5.22
Reflection Coefficient (dB)	**RT/duroid 6010.2LM**	-37	-21	-21	-53	-37	-21	-21	-53
	FR4	-21	-20	-21	-20	-20	-19	-20	-19

5.3 Measured Results

This section presents comparative analysis of measured and simulated results. The designed single and 8-element MIMO antenna system is fabricated on FR4 and RT/Duroid 6010.2LM substrates. The fabricated single element and 8-element MIMO antennas are shown in Fig. 5.10 (a-b) and 5.11(a-b) for FR4 and 6010.2LM respectively.

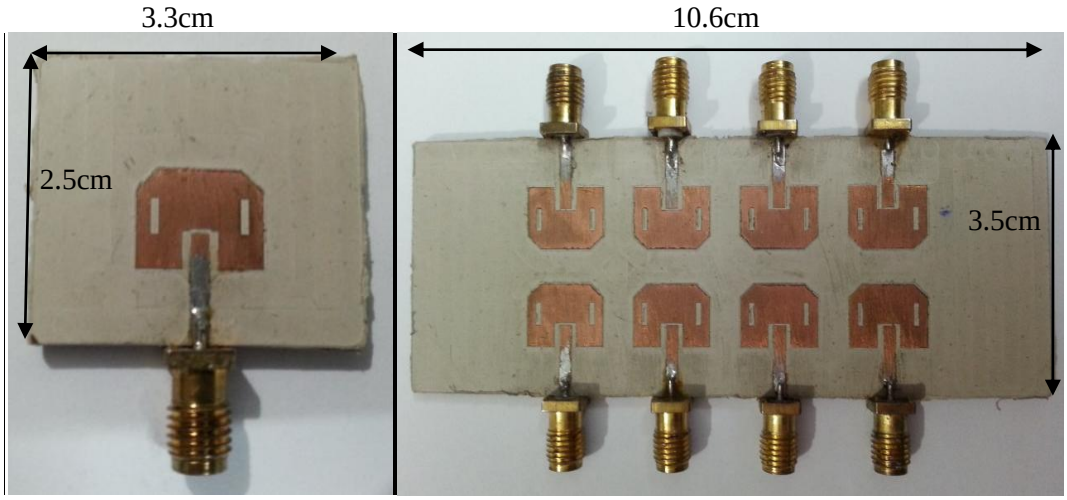

(a) (b)

Figure 5. 10: Fabricated antennas on RT/Duroid 6010.2LM (a) Single-element (b) 8-element MIMO array

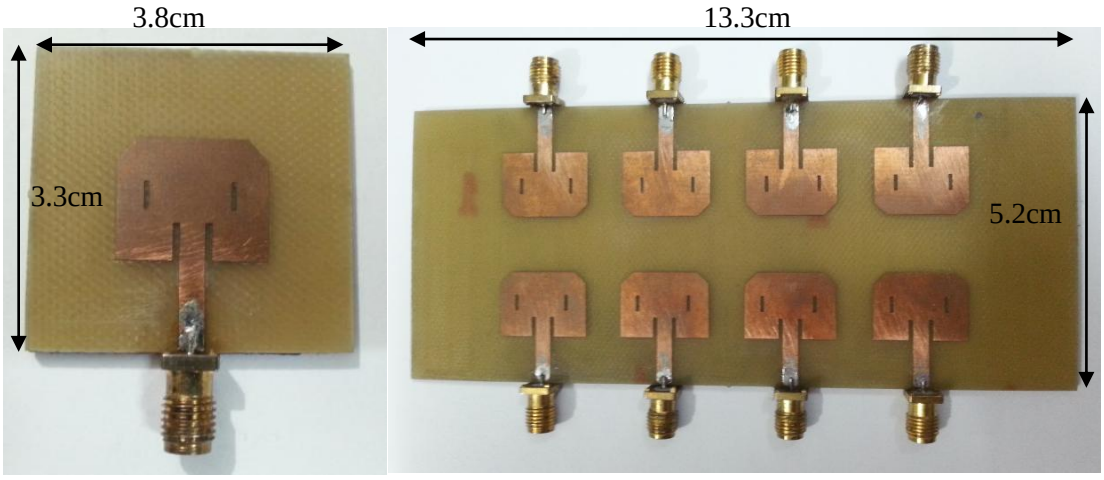

(a) (b)

Figure 5. 11: Fabricated antennas on FR4 (a) Single-element (b) 8-element MIMO array

5.3.1. Comparative Analysis of Measured and Simulation results (RT/Duroid 6010.2LM)

After fabrication, the reflection coefficients of the antennas were measured using the vector network analyzer (VNA). The VNA is a two-port network and is capable of measuring the S-parameters one-by-one for every single antenna element. Simulated and measured reflection coefficient curves of designed single and 8-element MIMO antenna array using RT/duroid 6010.2LM substrate is shown in Fig. 5.12 and Fig. 5.13(a-d) respectively. These plots depict that the measured return-loss and the bandwidth is almost identical to the simulated plot. The measured bandwidth of the fabricated single-antenna element is 192MHz whereas the bandwidth achieved for the 8-element MIMO antenna array is 171MHz. Results are also summarized in Table 10.

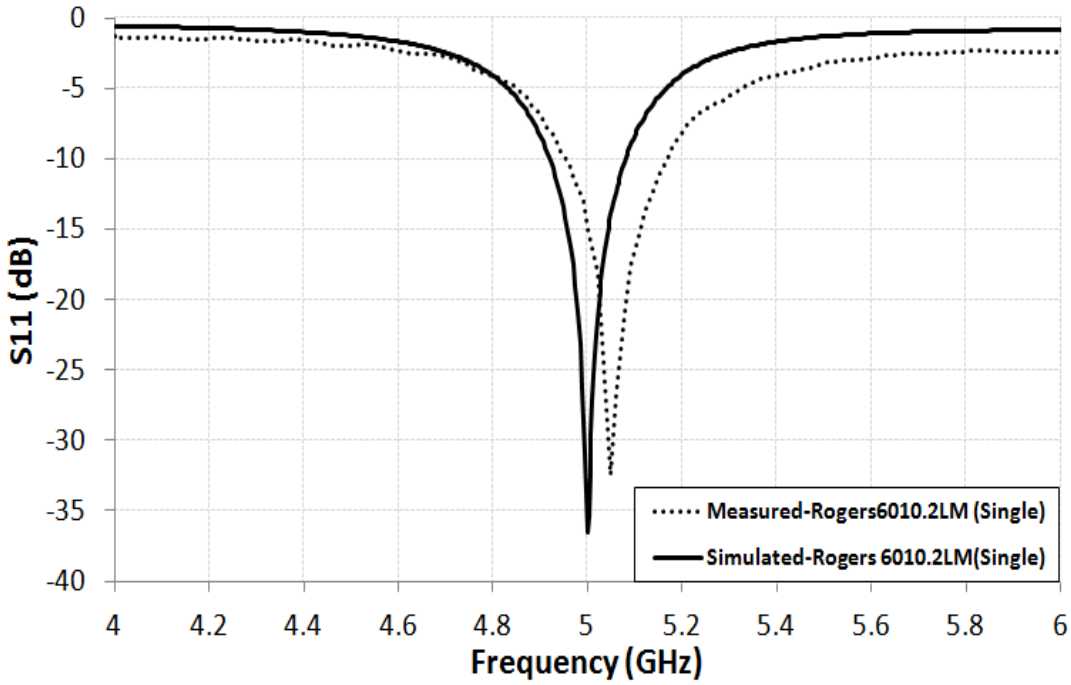

Figure 5. 12: Measured and simulated S_{11} of designed single-element MPA using RT/Duroid 6010.2LM

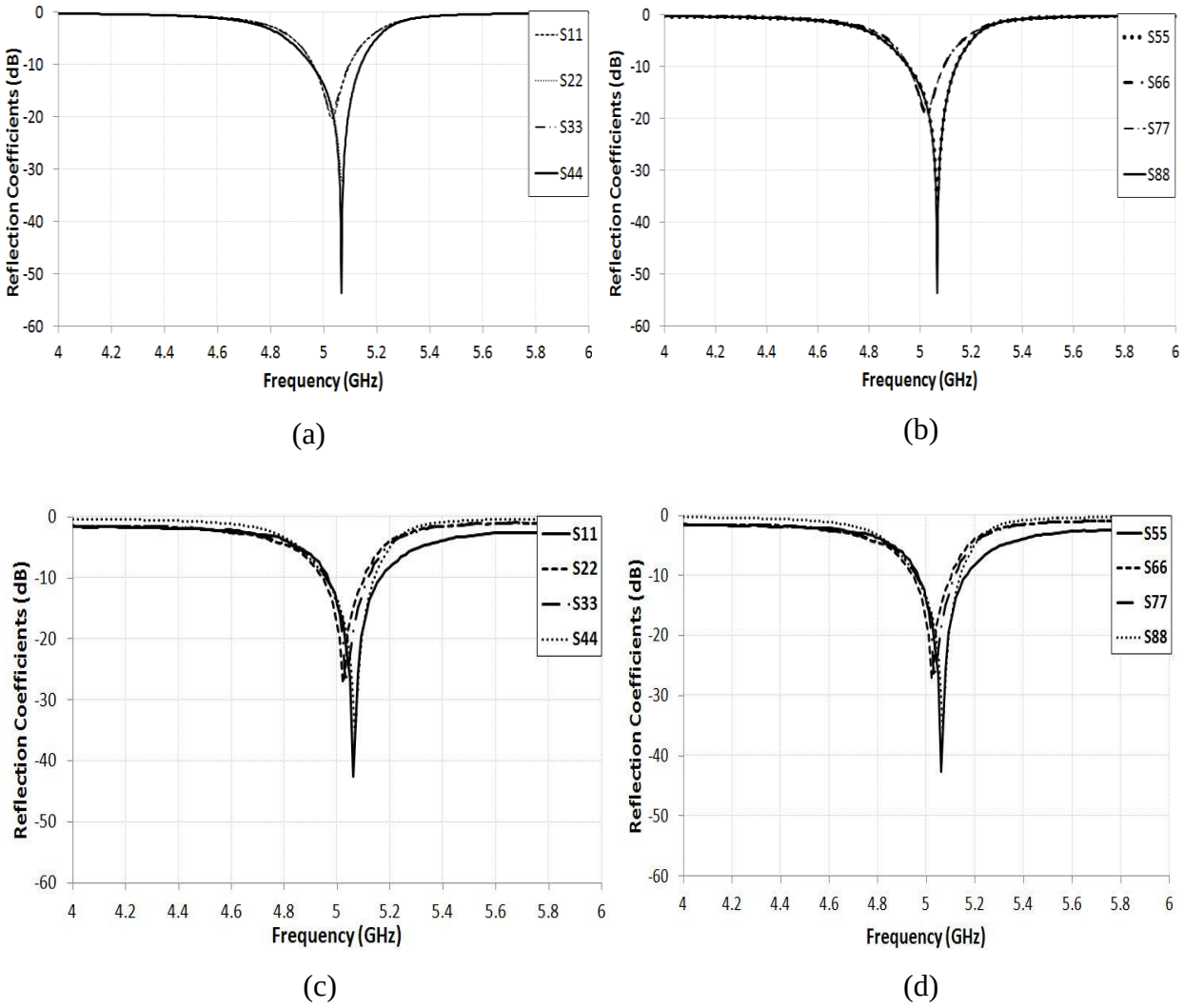

Figure 5. 13: Measured and simulated reflection coefficient of the designed 8-element MIMO antenna array on RT/Duroid 6010.2LM (a) Simulated– S_{11}-S_{44} (b) Simulated– S_{55}-S_{88} (c) Measured– S_{11}-S_{44} (d) Measured– S_{55}-S_{88}

5.3.2. Comparative Analysis of Measured and Simulation results (FR4)

The simulated and measured reflection coefficient curves of the designed single and 8-element MIMO antenna array using FR4 substrate is shown in Fig. 5.14 and Fig. 5.15(a-d) respectively. From these plots, it can be observed that the measured return-loss and the bandwidth is almost

similar to the simulated plot. The measured bandwidth of the fabricated single-antenna element is 210MHz whereas the bandwdith achieved for the 8-element MIMO antenna array is 180MHz.

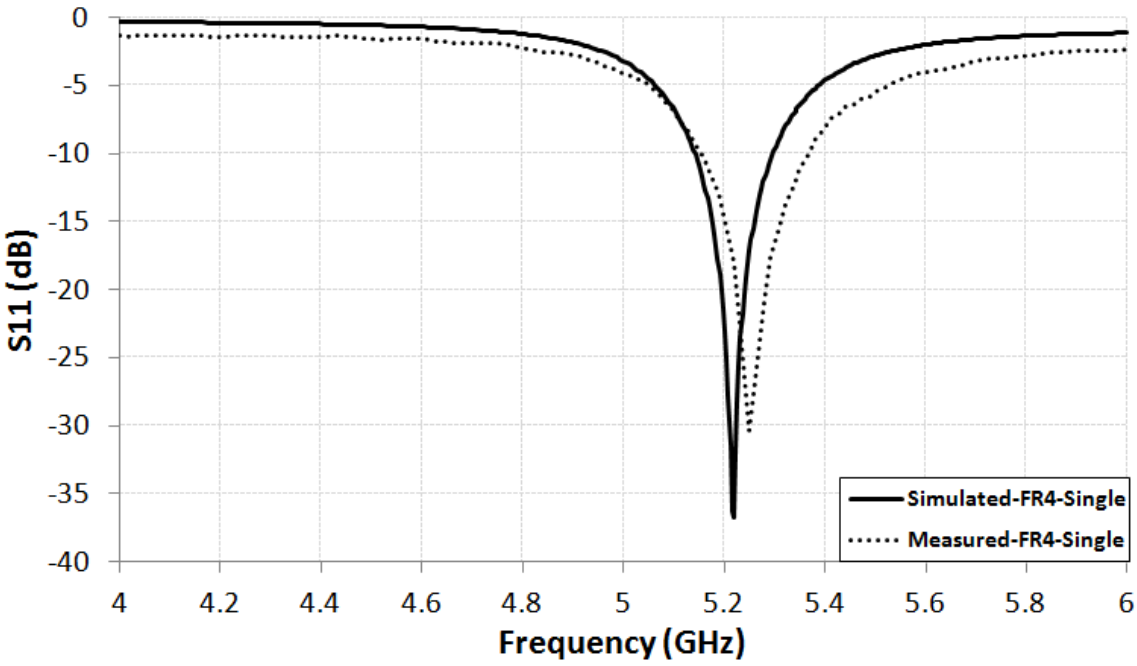

Figure 5. 14: Measured and simulated S_{11} of designed single-element MPA using FR4

The Fig. 5.15 (a-d) is shown on the next page for better comparison purposes. It is important to observe here in Fig. 5.15 (a-d) that the reflection coefficient curves S_{11}-S_{88} of the FR4 substrate based 8-element MIMO antenna array are not as good as the ones achieved by using the RT/Duroid 6010.2LM substrate which reflects to the performance comparison of a relatively lossy low-end substrate with a high-end Rogers substrate.

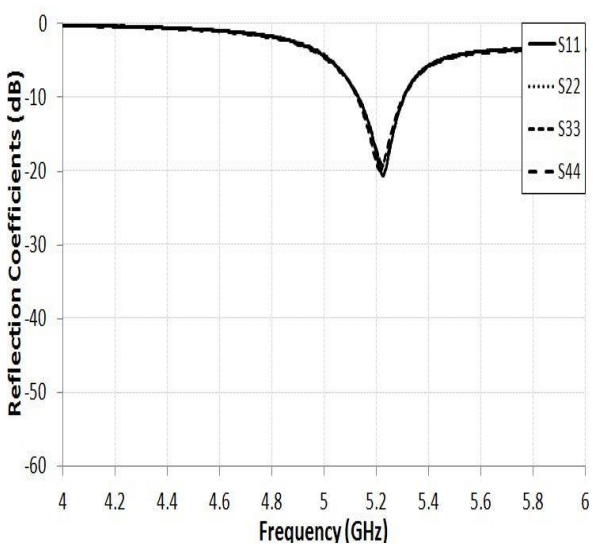

(a) Simulated– S_{11}-S_{44} (FR4)

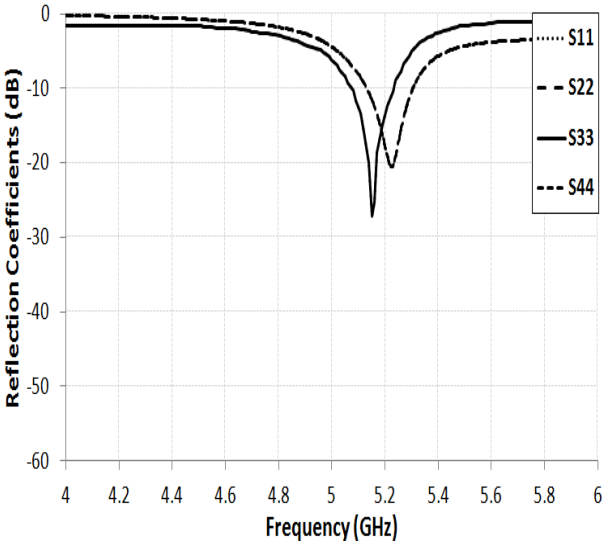

(b) Measured– S_{11}-S_{44} (FR4)

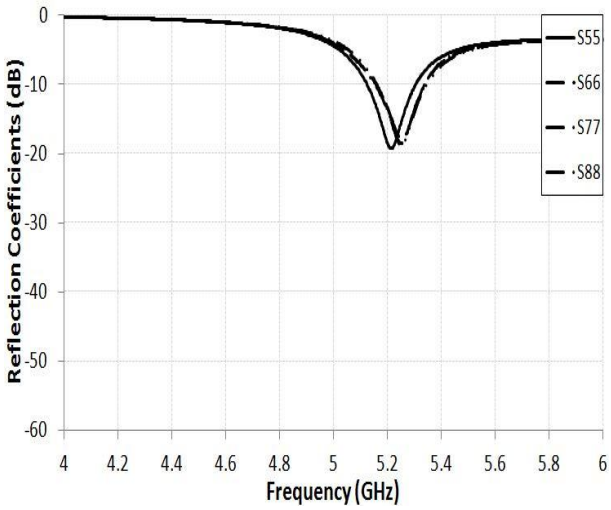

(c) Simulated– S_{55}-S_{88} (FR4)

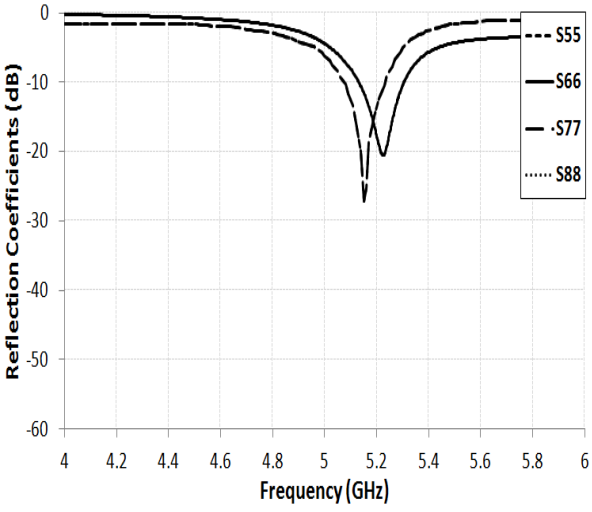

(d) Measured– S_{55}-S_{88} (FR4)

Figure 5. 15: Measured and simulated reflection coefficients of the designed 8-element MIMO antenna array on FR4 (a) Simulated– S_{11}-S_{44} (b) Measured− S_{11}-S_{44} (c) Simulated− S_{55}-S_{88} (d) Measured− S_{55}-S_{88}

The complete simulated and measured results comparison of the 8-element MIMO antenna array using both the RT/duroid 6010.2LM and FR4 substrates is given in Table 10 below.

Table 10: Comparison of measured and simulated results of the designed 8-element MIMO antenna array using RT/duroid 6010.2LM and FR4 substrates

2 x 4 MIMO Antenna Array for 802.11ac Wi-Fi applications									
			E_1	E_2	E_3	E_4	E_5	E_6	E_7	E_8
RT/duroid 6010.2LM	**Centre frequency (GHz)**	**Measured**	5.06	5.03	5.03	5.06	5.06	5.03	5.03	5.06
		Simulated (MoM)	5.07	5.02	5.02	5.07	5.07	5.02	5.02	5.07
	Reflection Coefficient (dB)	**Measured**	-43	-28	-28	-38	-44	-28	-28	-38
		Simulated (MoM)	-37	-21	-21	-53	-37	-21	-21	-51
FR4	**Centre frequency (GHz)**	**Measured**	5.17	5.22	5.17	5.22	5.17	5.22	5.17	5.22
		Simulated (MoM)	5.22	5.21	5.22	5.21	5.21	5.22	5.21	5.22
	Reflection Coefficient (dB)	**Measured**	-28	-21	-27	-21	-28	-21	-28	-20
		Simulated (MoM)	-21	-20	-21	-20	-20	-19	-20	-19

5.3.3. Radiation Pattern Measurements

The radiation pattern measurements of the fabricated antenna array were performed in the anechoic chamber [60].

5.3.3.1. RF Anechoic Chamber

A radio frequency anechoic chamber is a shielded room made to absorb all of the reflections of electromagnetic waves. Its internal walls are covered by a material which absorbs the incident radiation. The environment of an anechoic chamber simulates an open space of infinite dimensions, hence creating a free space. Its origin comes from a concept of stealth aircraft that that absorbs or scatters the radar waves. It provides an ideal environment to perform antenna radiation pattern measurements, radar and electromagnetic interference tests.

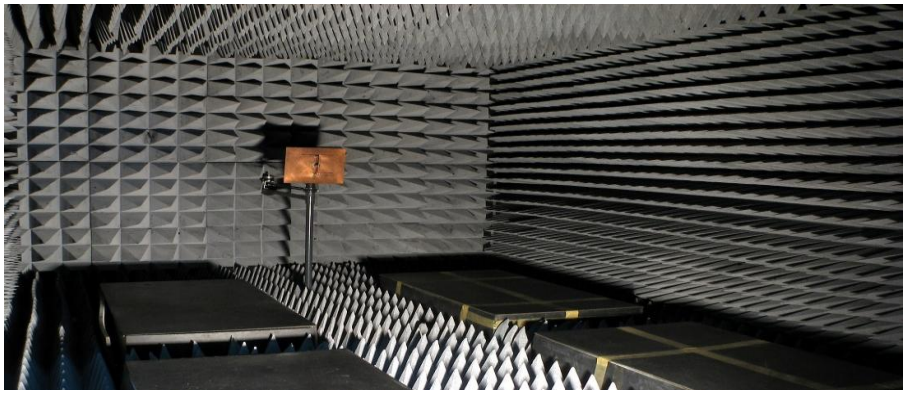

Figure 5. 16: RF anechoic chamber [60]

The absorbent material inside the anechoic chamber is called radiation absorbent material or RAM. The RAM is designed to effectively absorb every possible incident RF radiation coming from every possible direction. More efficient is the RAM less will be the RF reflections. The spurious radiation and reflection are ensured to be negligible and all internal surfaces are covered with RAM to avoid any measurement errors and ambiguities. The most widely used and effective type of RAM is pyramid shaped, arranged in arrays. These are made from a highly lossy material. To install some equipment inside the chamber, sections of RAM can be removed but must be replaced to perform any tests. RAM is made of a rubber-type foam material which consists of mixture of carbon and iron. This material is neither a good conductor nor a good electrical insulator because neither of them absorbs energy.

Figure 5. 17: Close view of Pyramidal RAM [60]

The RAM can be considered as a transmission line. In order to design RAM, we must first know how to design a transmission line with zero reflection. The walls of the chamber are metallic, so the terminals of the transmission line will be short circuited. The pyramid shape of the RAM attenuated the incident waves by scattering and absorption. The scattering occurs in foam structure where carbon particles promote destructive interference. The pyramid shape is formed in a way that maximizes the number of bounces that incident wave makes within the material. The wave loses its energy at each bounce and apparently disappearing. The permeability and permittivity of the RAM is complex which results in loss, as the wave pass through it. Usually, the RAM provides an attenuation rate of 11dB per centimeter [60].

The radiation pattern of all the antenna elements was measured and only one of them is shown here because all the elements are identical. Fig. 5.18(a) and (b) shows the 3D and 2D radiation pattern of the antenna at 5GHz frequency band for RT/Duroid 6010.2LM whereas 3D and 2D radiation patterns for FR4 are shown in Fig. 5.19(a) and (b) respectively. The intensity of the radio-frequency power on the pattern is shown by different colors. In Fig. 5.18(a) and 5.19(a) the red portion shows high intensity of power while yellow and green show comparatively low intensity.

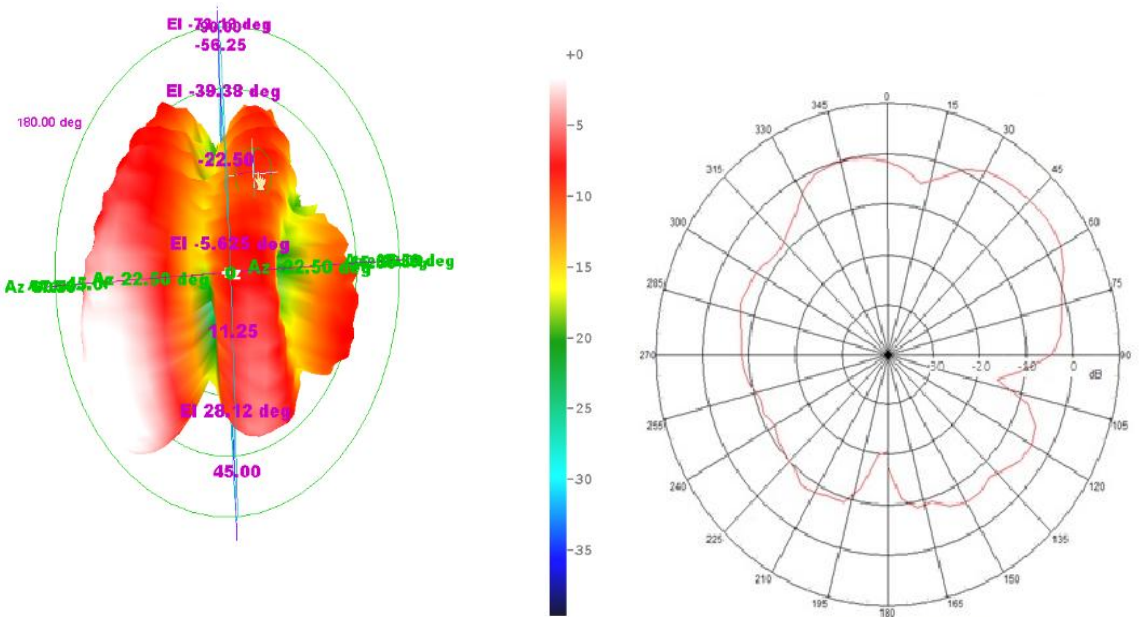

(a) (b)

Figure 5. 18: Measured radiation pattern of the fabricated antenna on Rogers 6010.2LM (a) 3D (b) 2D

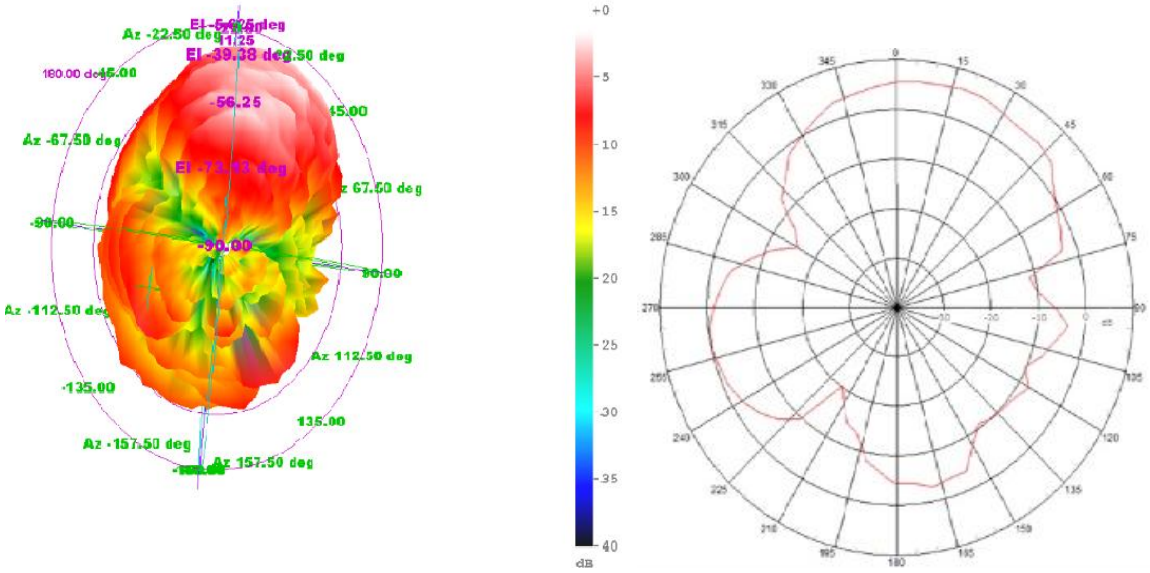

(a) (b)

Figure 5. 19: Measured radiation pattern of the fabricated antenna on FR4 (a) 3D (b) 2D

CHAPTER 6: CONCLUSION and FUTURE WORK

6.1. Conclusion

An efficient and compact 8-element MIMO antenna array design is proposed for next generation 802.11ac Wi-Fi applications that can operate at 5GHz WLAN band and facilitates the features that conform to 802.11ac Wi-Fi standard [1]. Initially, the antenna was designed on a substrate with high dielectric constant i.e. RT/duroid 6010.2LM and was simulated and verified on two different very well known software platforms i.e. ADS momentum and CST microwave studio to compare the performance of different modeling techniques i.e. MoM and FDTD. Both the techniques verified the design and resulted in desired frequency band being wide enough to meet the bandwidth requirement defined by IEEE 802.11ac Wi-Fi standard i.e. mandatory as 20-, 40-, and 80MHz and optional as 160MHz [2]. In the single-element antenna simulations, both platforms showed quite similar results but in case of MIMO antenna simulation, results achieved by MoM were better than the ones obtained by FDTD technique.

In order to evaluate the performance of a high and a low-end substrate i.e. Rogers 6010.2LM [51] and Flame Resistant 4 (FR4) [59], the 8-element MIMO antenna array for 802.11ac Wi-Fi application was also designed on FR4 substrate. It was observed that single element designed using both the substrates showed quiet similar outputs but, 8-element MIMO antenna array design showed better reflection coefficients when high dielectric substrate i.e. RT/Duroid 6010.2LM was used whereas low-end substrate i.e. FR4 resulted in better bandwidth than the one achieved with high-dielectric [51] substrate, which is due to the fact that substrates having low $\mathcal{E}_r$ and more thickness cause increase in bandwidth. The antennas were fabricated using both substrates i.e. RT/Duroid 6010.2LM and FR4 and their performance was compared against the simulated results. The measured results were found approximately similar to the

simulated results. The designed MIMO antenna system proposed in this paper can be integrated in any acute sized wireless device using WLAN in 5GHz band.

6.2. Future Recommendations

The work contributed in this research can serve as a guideline for the future research students who are interested in and have an innovative approach towards the field of smart antenna designing for real-life applications. Following research recommendations have been presented for further improvements in the proposed antenna.

- In future, beam-steering [8] and beam-forming [61] techniques may be applied using this type of MIMO antenna array in next generation WLANs.
- Similarly, the proposed MIMO antenna array operating at the 5GHz band can also be used in future deployments of radio-over-fiber (RoF) system remote antenna units by using the photonic active integrated antenna (PhAIA) concept [62].
- Moreover, other types of feeding networks can be incorporated to achieve better impedance matching.
- The 8-element MIMO antenna system should be tested in a real-world RF transmission / reception environment which leads to the better understanding of antenna performance etc.

References

[1] http://standards.ieee.org/news/2014/ieee_802_11ac_ballot.html

[2] Van Nee, R., "Breaking the Gigabit-per-second barrier with 802.11AC," Wireless Communications, IEEE , vol.18, no.2, pp.4,4, April 2011

[3] http://www.merunetworks.com/gated-pages/idc-tech-brief.html

[4] Nojima, D.; Lanante, L.; Nagao, Y.; Kurosaki, M.; Ochi, H., "Performance evaluation for multi-user MIMO IEEE 802.11ac wireless LAN system," *Advanced Communication Technology (ICACT), 2012 14th Int. Conf. on*, , pp.804-808, Feb. 2012

[5] M. A. Jensen and J. W. Wallace, "A review of antennas and propagation for MIMO wireless systems," *IEEE Trans. Antennas Propagat*., vol. 52,no. 11, pp. 2810–2824, Nov. 2004.

[6] Muhsin Ali, Khawaja Bilal Ahmed Mahmood, Microstrip Patch Antenna Array For LTE AND MIMO Applications, Lambert Academic Publishing (LAP), 2014, ISBN: 384841418X, 9783848414185

[7] Constantine A. Balanis "Antenna Theory", 3rd edition, ISBN: 978-0- 471-66782-7

[8] A. Paulraj, D. Gore, R. Nabar, and H. Bolcskei, "An overview of MIMO communications - a key to gigabit wireless," Proceedings of the IEEE, vol. 92, no. 2, pp. 198 – 218, Feb. 2004.

[9] Verma, L.; Fakharzadeh, M.; Sunghyun Choi, "Wifi on steroids: 802.11ac and 802.11ad", *Wireless Communications, IEEE*, vol.20, no.6,pp. 30-35, Dec 2013

[10] Eng Hwee Ong; Kneckt, J.; Alanen, O.; Zheng Chang; Huovinen, T.;Nihtila, T., "IEEE 802.11ac: Enhancements for very high throughput WLANs," *Personal Indoor and*

Mobile Radio Communications (PIMRC), IEEE 22nd Int. Symp. on, pp. 849-853, Sept. 2011

[11] http://electronicdesign.com/communications/understanding-ieee-80211ac-vht-wireless

[12] Altman, Zwi; Wiart, Joe; Mittra, Raj. 1998. Design of high gain dipole antennas using the genetic algorithm. IEEE Antennas and Propagation Society International Symposium. 1998. Volume 1. Pages 30-33.

[13] Msc. Thesis, "Design and Simulation of Microstrip Phase Array Antenna using ADS," Linnaeus University, 2011.

[14] Stutzman, W.L. and Thiele, G.A., Antenna Theory and Design, John Wiley & Sons, Inc, 1998.

[15] N. J. Kolias, R. C. Compton, J. P. Fitch and D. M. Pozar, Antenna, CRC Press, 2000.

[16] Saunders, S.R., Antennas and Propagation for Wireless Communication Systems, John Wiley & Sons, Ltd, 1999.

[17] John D. Kraus and Ronald J. Marhefka, "Antennas: For All Applications, Third Edition", 2002, McGraw-Hill Higher Education.

[18] Makarov, S.N., Antenna and EM Modeling with MATLAB, John Wiley & Sons, Inc, 2002.

[19] http://www.comsol.com/blogs/2d-axisymmetric-model-conical-horn-antenna

[20] Sharawi, Mohammad S. "A 5-GHz 4/8-element MIMO antenna system for IEEE 802.11AC devices." Microwave and Optical Technology Letters 55.7 (2013): 1589-1594. Print.

[21] Bianchi, G. "IEEE 802.11-saturation throughput analysis." IEEE COMMUNICATIONS LETTERS 2.12 (1998): 318-320. Print.

[22] Bejarano, Oscar, Edward W. Knightly, and Minyoung Park. "IEEE 802.11ac: from channelization to multi-user MIMO." IEEE Communications Magazine 51.10 (2013): 84-90. Print.

[23] B. Boris, J. Barcelo, D. Staehle, A. Vinel, and M. Oliver. "On the Performance of Packet Aggregation in IEEE 802.11ac MU-MIMO WLANs." IEEE COMMUNICATIONS LETTERS 16.10 (2012): 1588-1591. Print.

[24] http://www.radio-electronics.com/info/wireless/wi-fi/ieee-802-11-standards-tutorial.php

[25] http://www.dailywireless.org/2013/06/19/wifi-alliances-announces-802-11ac-certification-program/

[26] http://www.motorolasolutions.com/web/Business/_Documents/White%20Paper/Static%20files/ 80211ac_White_Paper_0712-web.pdf

[27] Cheng-Xiang Wang; Haider, F.; Xiqi Gao; Xiao-Hu You; Yang Yang; Dongfeng Yuan;Aggoune, H.; Haas, H.; Fletcher, S.; Hepsaydir, E., "Cellular architecture and key technologies for 5G wireless communication networks," *Communications Magazine, IEEE*, vol.52, no.2, pp. 122-130, Feb 2014

[28] http://www.newegg.com/Product/Product.aspx?Item=N82E16833315123

[29] A Erel, M., "Design of Microstrip Patch Antenna for the NPSAT1" , ISBN: 1423505670, 978142350567,Storming Media, 2002

[30] VanHese J, Sercu J, Pissoort D, Lee H-S, "State of the Art in EM Software for Microwave Engineers": Keysight Technologies Application Note 5990-3225EN, February 2009

[31] http://literature.cdn.keysight.com/litweb/pdf/5990-9759EN.pdf

[32] Kumar, G. and Ray, K.P., Broadband Microstrip Antennas, Artech House, Inc, 2003.

[33] Bahl, I.J. and Bhartia, P., Microstrip Antennas, Artech House, Dedham, MA, 1980.

[34] F. Croq, *et al.*, "Stacked resonators for bandwidth enhancement: a comparison of two feeding techniques," *Microwaves, Antennas and Propagation, IEE Proceedings H*, vol. 140, pp. 303-308, 1993.

[35] L. Kai-Fong, *et al.*, "Circular-disk microstrip antenna with an air gap," *Antennas and Propagation, IEEE Transactions on*, vol. 32, pp. 880-884, 1984.

[36] C. Wood, "Improved bandwidth of microstrip antennas using parasitic elements," *Microwaves, Optics and Antennas, IEE Proceedings H*, vol. 127, pp. 231-234, 1980.

[37] G. Kumar and K. Gupta, "Nonradiating edges and four edges gap-coupled multiple resonator broad-band microstrip antennas," *Antennas and Propagation, IEEE Transactions on*, vol. 33, pp. 173-178, 1985.

[38] Nasir, S.A.; Arif, S.; Mustaqim, M.; Khawaja, B.A., "A log-periodic microstrip patch antenna design for dual band operation in next generation Wireless LAN applications," (ICET), 2013 IEEE 9th International Conference on *Emerging Technologies*, , pp.1-5, Dec.2013.

[39] W. H. Hsu, and Wong , K.L, "Broadband Aperture Coupled shorted patch antenna."

[40] M. Luk, Mak, C.L. Chow, Y.L. and Lee K.K, "Broadband microstrip patch antenna."

[41] S. S. Thorat, R.C. Jaiswal, D. Rajkumar, S. D. Lokhande, 'Efficient technique for Bandwidth Improvement of Mictrostrip Patch Antenna", *IRACST – Int.l Journal of Computer Networks and Wireless Communications (IJCNWC), Vol.2, No6,* Dec 2012

[42] T. Huynh and K. F. Lee, "Single-layer single-patch wideband microstrip antenna," *Electronics Letters*, vol. 31, pp. 1310-1312, 1995.

[43] Noor, Asadullah. "Design of microstrip patch antennas at 5.8 Ghz." (2012).

[45] Hammerstad, E.O., "*Equations for Microstrip Circuit Design*," Proc. Fifth European Microwave Conf., pp. 268-272, September 1975.

[46] James, J.R. and Hall, P.S., Handbook of Microstrip Antennas, Vols 1 and 2, Peter Peregrinus, London, UK, 1989.

[47] Garg, R., Bhartia, P., Bahl, I., Ittipiboon, A., Microstrip Antenna Design Handbook, Artech House, Inc, 2001.

[48] Arif, S.; Nasir, S.A.; Mustaqim, M.; Khawaja, B.A., "Dual U-slot triple band microstrip patch antenna for next generation wireless networks," *Emerging Technologies (ICET), 2013 IEEE 9th International Conference on* , vol., no., pp.1,6, 9-10 Dec. 2013

[49] Advanced Design System, 2008 Momentum Software Manual, Agilent Technologies, CA: Palo Alto, 2008.

[50] https://www.cst.com/Content/Media/cst-studio-suite-2012-brochurelow.pdf

[51] http://www.rogerscorp.com/documents/612/acm/RT-duroid-6006-6010LM-laminate-data-sheet.pdf

[52] Ali, Z.; Singh, V.K.; Singh, A.K.; Ayub, S., "Wide Band Inset Feed Microstrip Patch Antenna for Mobile Communication," *Communication Systems and Network Technologies (CSNT), 2013 International Conference on* , vol., no., pp.51,54, 6-8 April 2013

[53] V. Natarajan, D. Chatterjee, "*An Empirical Approach for Design of Wideband, Probe-fed, U-slot Microstrip Patch Antennas on Single-layer, Infinite, Grounded Substrates*," ACES Journal, vol. 18, no. 3, November 2003.

[54] Dongkeun Jung; Yunjin Woo; Cheunsoo Ha, "Modified inset fed microstrip patch antenna," Microwave Conference, 2001. APMC 2001. 2001 Asia-Pacific , vol.3, no., pp.1346,1349 vol.3, 2001

[55] Aanandan, C.K.; Mohanan, P.; Nair, K.G., "Broad-band gap coupled microstrip antenna," Antennas and Propagation, IEEE Transactions on , vol.38, no.10, pp.1581,1586, Oct 1990

[56] Khan, M.U.; Sharawi, M.S., "A compact 8-element MIMO antenna system for 802.11ac WLAN applications," *Antenna Technology (iWAT), 2013 International Workshop on*, pp.91-94, Mar 2013

[57] Abdulla A. Abouda and S.G. Häggman,"Effect of Mutual Coupling on Capacity of MIMO Wireless Channels in High SNR Scenario,"*Progress In Electromagnetic Research PIER* 65, pp. 27-40, 2006.

[58] Pan, S, Durrani, S & Bialkowski, M 2007, 'MIMO Capacity for Spatial Channel Model Scenarios', *Australian Communications Theory Workshop (AusCTW 2007)*, , Adelaide Australia, pp. 25-29.

[59] https://atlas-proj-tgc.web.cern.ch/atlas-proj-tgc/TGC_cons_DS.pdf

[60] Holloway, DeLyser, German, McKenna & Kanda, "*Comparison of Electromagnetic Absorber Used In Anechoic and Semi-Anechoic Chambers For Emissions and Immunity Testing of Digital Devices*," IEEE Transactions on Electromagnetic Compatibility, February, 1997.

[61] W. Roh *et al.*, " Millimeter-wave beamforming as an enabling technology for 5G cellular communications: theoretical feasibility and prototype results", *IEEE Communications Magazine*, Vol. 52, No.2, pp. 106 - 113, Feb 2014

[62] B. A. Khawaja, M. J. Cryan, "Millimetre-wave photonic active integrated antennas (PhAIAs) using hybrid mode-locked lasers", *Microw. Opt. Technol. Lett.* 54 (5), pp. 1200–1203 (2012)

[63] http://9to5mac.com/2012/07/25/broadcom-announces-bcm4335-chip-that-will-likely-power 2013s-ipad-and-iphone-to-gigabit-5g-wifi/

[64] IEEE Standard Definitions of Terms for Antennas," *IEEE Std 145-1983* , vol., no., pp.1,31, June 22 1983

[65] V. V. Thakare and P. K. Singhal, "Bandwidth analysis by introducing slots in microstrip antenna design using ANN," *Progress In Electromagnetics Research M*, Vol. 9, 107-122, 2009.